

Article

Adsorption of Wormlike Chains onto Partially Permeable Membranes

Alexander Semenov * and Irina Nyrkova

Institut Charles Sadron, CNRS-UPR 22, University of Strasbourg, CEDEX 2, 67034 Strasbourg, France

* Correspondence: al.ni.semenov@gmail.com

Abstract: Reversible adsorption of a single stiff wormlike macromolecule to flat membranes with various permeabilities is considered theoretically. It is shown that the adsorbed layer microstructure is significantly different from either a flexible chain or a stiff chain adsorption at a solid surface. Close to the critical point, the adsorbing wormlike chain forms a strongly anisotropic proximal layer near the membrane in addition to a nearly isotropic distal layer. The proximal layer is characterized by the algebraic monomer concentration profile, $c(x) \propto |x|^{-\beta}$, due to the self-similar distribution of aligned polymer loops. For a perfectly penetrable membrane, $\beta = 1$ which is different from $\beta = 4/3$ obtained for semiflexible chain adsorption at a solid surface. Moreover, we establish that the critical exponent for a partially permeable membrane depends on its properties (porosity w) and propose an asymptotically exact theory (based on the generalized Edwards equation) predicting this dependence, $\beta = \beta(w)$. We also develop a scaling theory elucidating, in particular, an intricate competition of loops and tails in both proximal and distal sublayers.

Keywords: adsorption; polymers; membranes

1. Introduction

Polymer adsorption is a remarkable phenomenon relevant to many applications [1–4]. It is routinely used to modify surface properties by coating with adsorbed polymer layers for protection, lubrication and adhesion, and to tune the physical properties of interfacial functional layers. Adsorption from a solution can efficiently impart the stabilization of colloidal and nano-particles (including protein complexes), preventing their aggregation [1,2,5–7]. Single-chain adsorption is involved in many biological processes [8–11].

Both equilibrium properties and kinetics of flexible polymer adsorption have been studied theoretically since long ago [3,4]. Typically, polymer adsorption is caused by short-range monomer–surface interactions (of strength u). For flexible polymers, it was established that single-chain adsorption is akin to a critical phenomenon (a second-order phase transition), where the order parameter p (the fraction of monomers in contact with the attractive surface) changes in a continuous way, becoming nonzero beyond the critical threshold u^* (at $u > u^*$) in the limit $N \rightarrow \infty$, where N is the number of monomers in the chain [4,12]. Exactly at $u = u^*$, the number of surface contacts $n_c = Np$ scales as

$$n_c \propto N^\phi \quad (1)$$

where ϕ is the crossover exponent [4,12,13]. The polymer concentration profile $c(x)$ at $u = u^*$ near the surface follows the critical scaling law, $c(x) \propto x^{-\beta}$, where x is the distance to the surface. For $\phi < 1$, the exponent β is also smaller than 1 and is related to ϕ : $\beta = 1 - \frac{1-\phi}{\nu}$, where ν is the exponent defining the size (gyration radius R_G) of an isolated coil, $R_G \propto N^\nu$. In a good solvent, $\phi \approx 0.485$ [14–16] and $\nu \approx 0.588$ [17], so $\beta \approx 0.124$, while in Θ -solvent (or marginal solvent) polymer coils follow the ideal-chain statistics (apart from logarithmic corrections) [4], so $\nu = 0.5$, $\phi = 0.5$ and $\beta = 0$.



Citation: Semenov, A.; Nyrkova, I. Adsorption of Wormlike Chains onto Partially Permeable Membranes. *Polymers* **2023**, *15*, 35. <https://doi.org/10.3390/polym15010035>

Academic Editor: Vladimir Shelukhin

Received: 28 November 2022

Revised: 16 December 2022

Accepted: 17 December 2022

Published: 22 December 2022



Copyright: © 2022 by the authors. Licensee MDPI, Basel, Switzerland. This article is an open access article distributed under the terms and conditions of the Creative Commons Attribution (CC BY) license (<https://creativecommons.org/licenses/by/4.0/>).

One of the most important characteristics of macromolecules is their backbone stiffness, which is related to the correlation length l_p of the chain orientation along its contour. Stiff polymers have large persistence length l_p , which is much longer than their thickness d : $l_p/d \gg 1$. Many physical and, in particular, adsorption properties of such semirigid (or semiflexible) macromolecules are significantly different [18–23] from those of flexible chains (whose l_p is comparable to d). The family of stiff polymers is wide: it includes synthetic helical polymers (such as poly- γ -benzyl-L-glutamate), polyelectrolytes, and important biological polymers, such as double-strand DNA, polypeptides and proteins, microtubules, F-actin and other protein polymers (biofilaments). By far, the most used statistical model of semirigid polymers is the wormlike chain (Kratky–Porod) model [8,18,21,24]. The model is also applicable to biopolymers [25]. For example, as pointed out in ref. [10], on length scales smaller than the Kuhn segment length, accessible by scanning force microscopy, conformations of a single DNA molecule were shown [26] to be appropriately described by the wormlike chain model. (Some recently reported deviations [23] from the wormlike chain behavior for some biopolymers only confirm the central role of the Kratky–Porod model). This model is adopted here; it implies that the orientational correlations along the chain contour decay exponentially with the curvilinear (contour) distance s :

$$\langle \underline{n}(s+s') \cdot \underline{n}(s') \rangle = e^{-s/l_p} \quad (2)$$

where $\underline{n}(s')$ and $\underline{n}(s+s')$ are unit vectors tangential to the backbone at points s' and $s+s'$, respectively. The mean-square end-to-end distance of a *long* persistent (wormlike) chain is

$$R^2 \simeq lL \quad (3)$$

where $l = 2l_p$ is Kuhn segment of the chain, and $L \gg l$ is its contour length. In the opposite regime, $L \ll l$, we trivially have $R \simeq L$.

Back in 2002, we considered the adsorption of a semiflexible wormlike chain at a solid surface [21]. It was shown that while the adsorption transition is continuous, it becomes progressively sharper as the chain rigidity increases. In particular, the fraction of adsorbed monomers (in a thin layer of thickness $\sim \Delta$ within the surface attractive potential range) jumps from nearly 0 to almost 1 in a narrow temperature range (around the critical point) whose relative width is proportional to $(\Delta/l)^{4/3}$, where l is the Kuhn segment of the chain. In this respect, the adsorption transition becomes similar to a first-order phase transition. It was also shown [21] that at the critical point, the polymer concentration follows the specific scaling law, $c(x) \propto x^{-4/3}$ for $\Delta \lesssim x \lesssim l$.

In the present paper, we analyze the adsorption of wormlike macromolecules to a thin free-standing film, such as a membrane or a giant surfactant vesicle, or a lipid bilayer. It may seem that adsorption onto a film is similar to the solid surface case. However, the main difference from the previously considered case is that now, we take into account that the film can be (at least, partially) penetrable for the adsorbing chain.

In the next section, we consider the adsorption of a short polymer chain (with $L \lesssim l$) to a perfectly penetrable membrane. First, we present a scaling argument predicting the critical strength u^* of polymer/membrane attraction required for adsorption. Next we develop a scaling theory for polymer statistics at the adsorption threshold ($u = u^*$) and slightly below ($u < u^*$) or above it. The u -dependencies of the energy E (which is proportional to the fraction p of adsorbed polymer segments located within the membrane attraction range) and the adsorption free energy F are considered there as well. In Section 3, we develop a quantitative approach to analyze the adsorption microstructure, using the generalized Edwards equation. The theory is focused on the proximal layer (of thickness $\lesssim l$) formed by long chains at $u = u^*$. A more general case, $u \neq u^*$, is considered in Section 4 based on scaling arguments. The relevant experimental systems are discussed in Section 5. The adsorption of a semiflexible wormlike polymer to partially penetrable porous membranes (solid films with holes) is then studied in detail in Section 6. The main results are discussed and summarized in Sections 7 and 8, respectively.

2. Perfectly Penetrable Free-Standing Film

2.1. Adsorption Threshold

We start with the simplest model, ignoring any internal structure of the film (membrane), which is represented just by a potential near the film (located at the plane $x = 0$):

$$U(x) = -Tu\varphi(|x|/\Delta) \quad (4)$$

where $U(x)$ is the potential energy *per unit length* of the chain, T is the temperature in energy units ($T = k_B T_{abs}$ with T_{abs} , the absolute temperature), u is the energy parameter, Δ is microscopic length defining the potential range, and φ is a non-dimensional function specifying a fast decay of the potential with the distance $|x|$ from the film. In the simplest case, the potential shape is rectangular: $\varphi = 1$ for $|x| < \Delta$, and $\varphi = 0$ otherwise.

It is always assumed that the chain is sufficiently rigid, $l \gg \Delta$, and that its contour length L is large, $L \gg \lambda$, where the microscopic length-scale λ is defined below (cf. Equation (7)). In this case, the wormlike chain gets strongly trapped near the film for $u > u^*$, where u^* is the adsorption threshold, which is defined mainly by l and Δ (and, strictly speaking, also by the function $\varphi(x)$). It can be estimated as

$$u^* \sim 1/(\Delta^2 l)^{1/3} \quad (5)$$

A similar estimate was obtained for the case of adsorption to an impenetrable surface [18,21,27]. The result, Equation (5), can be deduced from two statements: If $u \gg u^*$ the chain must be localized near the adsorbing plane. By contrast, for $u \ll u^*$ the chain statistics are just weakly affected by the adsorbing potential (provided that the chain is not too long). Both statements are justified below: Let us consider a chain fragment with one end located at $x = 0$ and oriented parallel to the plane. By virtue of the wormlike flexibility implied by the Kratky–Porod chain model [24] adopted here (note that most of semirigid polymers are well-described by this model), the tangential vector $\underline{n} = \underline{n}(s)$ gradually changes along the chain contour (here s is the curvilinear coordinate). The typical angle between $\underline{n}(s)$ and the adsorbing plane is $\theta(s) \sim (s/l)^{1/2}$ for $s \ll l$ [18,21,22]. (Note that θ is also the typical angle between $\underline{n}(0)$ and $\underline{n}(s)$ as follows from Equation (2)). The corresponding typical deviation along the x -axis is

$$x(s) \sim s\theta(s) \sim s^{3/2}/l^{1/2} \quad (6)$$

Once $x(s)$ exceeds the attraction length Δ , a correction to the chain trajectory is required in order to keep the chain in the Δ -layer, which costs about the thermal energy T . The corresponding fragment length is $s \sim \lambda$, where

$$\lambda \sim l^{1/3}\Delta^{2/3} \quad (7)$$

is the relevant microscopic length-scale along the chain. The whole chain confinement free energy (entropic cost) is, therefore, $F_{conf} \sim TL/\lambda$, while its attraction (potential) energy is $E \sim -TLu$. Therefore, the total adsorption free energy $F = F_{conf} + E$ is negative for $u \gg u^* \sim 1/\lambda$, and hence the chain confinement in the Δ -layer (i.e., in the region $-\Delta < x < \Delta$ where polymer/membrane attraction is significant) is favorable in this case.

To justify the second statement, it is sufficient to estimate the upper bound for the total interaction energy, assuming that one chain end is pinned in the Δ -layer being oriented tangentially to it. The probability that a point s of the chain ($s \gtrsim \lambda$) is inside the Δ -layer is $p(s) \sim \Delta/x(s)$. On using Equations (6) and (7) for $\lambda \lesssim s \lesssim l$ we therefore obtain

$$p(s) \sim l^{1/2}\Delta/s^{3/2} \sim (\lambda/s)^{3/2} \quad (8)$$

Obviously $p(s) \sim 1$ for $s \lesssim \lambda$. For $s \gtrsim l$ the chain is nearly Gaussian, so $x(s) \sim l(s/l)^{1/2}$ and $p(s) \sim \Delta/(sl)^{1/2}$. The total interaction energy is therefore

$$E \sim -uT \int_0^L p(s)ds \sim -uT(\lambda + \sqrt{L/l}\Delta)$$

The chain interactions with the adsorbing membrane can be neglected if $E/T \ll 1$; this condition is valid (in the regime $u \ll u^*$) provided that

$$L \lesssim l(l/\Delta)^{2/3} \equiv L_m \tag{9}$$

Note that $L_m \gg l$. In the next subsections, we consider the adsorption of relatively short, stiff, wormlike polymers with $L \lesssim l$; both Equations (5) and (9) are valid in this case. Moreover, as discussed in Section 4, Equation (5) is generally valid, provided that u^* is properly interpreted as the critical point for strongly anisotropic adsorption.

2.2. Adsorbed Layer Structure and Concentration Profile

Below, we build a scaling picture of a polymer layer critically adsorbed to a penetrable film for the case $\lambda \ll L \lesssim l$. Longer chains ($L \gg l$) are considered in Sections 3, 4 and 6. Generally, exactly at the adsorption threshold $u = u^*$, the chain is not yet trapped by the adsorbing surface (since the net free energy gain per segment is close to zero at $u = u^*$, see discussion in Section 7), so it is useful to demand that both ends of the chain are located in the attraction Δ -layer and are oriented parallel to it (to avoid their escape into the bulk of the solution). In this case, the layer can be viewed as a system of trains and loops: the trains are fragments of length $s_{train} \gtrsim \lambda$ located entirely in the Δ -layer, and the loops are the fragments between the trains (see Figure 1a). Note that the typical angle between any train segment and the membrane plane is

$$\theta_\Delta = (\lambda/l)^{1/2} \sim (\Delta/l)^{1/3} \tag{10}$$

It is important that loops can intersect the Δ -layer, but each intersecting fragment (labeled as ‘int’ in Figure 1a) is short: its length $s_{int} \ll \lambda$ (otherwise, this fragment would be considered as a train), so the energy of each intersection E_{int} is small, $|E_{int}| \ll T$. It is, therefore, plausible to assume that interactions with the Δ -layer just weakly perturb the statistics of a loop, which remains (nearly) ideal. To prove that this assumption is self-consistent, let us estimate the total interaction energy E_{int}^{tot} of a single loop of length s . Reiterating the argument given at the end of Section 2.1, we obtain (cf. Equation (8))

$$E_{int}^{tot}(s) \sim -2uT \int_0^{s/2} p(s)ds \sim T$$

The partition function of a loop, $Z_l(s)$, $s \gg \lambda$, must be therefore of the same order as that of an ideal loop whose segments do not interact with the film. The latter can be estimated as just the probability $P(s)$ that an s -fragment starting in Δ -layer with initial orientation $\theta(0) \sim \theta_\Delta$ has its end-point in the same layer with a similar orientation: $x \sim \Delta$, $\theta \sim \theta_\Delta$ at the end point. Recalling that the typical unconstrained values are much larger, $x(s) \gg \Delta$, $\theta(s) \gg \theta_\Delta$, for $s \gg \lambda$ (cf. Equation (6)), we obtain $P(s) \sim \theta_\Delta \Delta/[x(s)\theta(s)]$.

Therefore,

$$Z_l(s) \sim P(s) \sim \frac{l^{1/2}\Delta \lambda^{1/2}}{s^{3/2} s^{1/2}} \sim \frac{\lambda^2}{s^2} \tag{11}$$

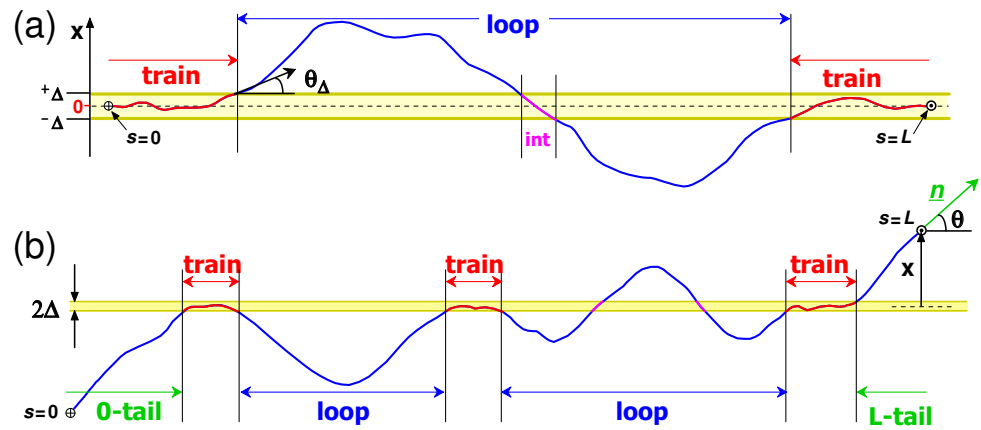


Figure 1. (a) A wormlike chain with two ends located in the membrane (at $-\Delta < x < \Delta$). The chain segments are oriented at small angles θ to the membrane plane ($x = 0$). Typically, $|\theta| \lesssim \theta_\Delta$ in the ‘train’ sections, and $|\theta| \gg \theta_\Delta$ in the ‘loops’ (see Equation (10)). (b) A wormlike chain of contour length L with free ends; the chain is aligned by attraction to a penetrable membrane. The right-hand end is located at distance x from the membrane mid-plane; its orientation is defined by the unit vector \underline{n} . The chain involves ‘train’ sections trapped in the short-range attraction layer representing the membrane, ‘loops’ of different sizes away from it, and two ‘tails’.

The above scaling law is applicable to loops with $s \gg \lambda$, while shorter loops with $s \sim \lambda$ are similar to trains. We therefore arrive at a self-similar distribution of loops: the number density of loops of size s is proportional to $Z_l(s)$. The concentration profile can be obtained using Equation (11) and the following argument was already employed in refs. [21,23]: The polymer concentration at the distance $x \gg \Delta$ from the membrane is defined by loops of such length s that $x(s) \sim x$, i.e., $s \sim \lambda(x/\Delta)^{2/3}$. The number of monomers in such loops is $\sim \int_{s/2}^s s' Z_l(s') ds' \sim s^2 Z_l(s)$ which must be proportional to $\int_{x/2}^x c(x') dx' \sim xc(x)$. As $s^2 Z_l(s) = \text{const}$, we obtain

$$c(x) \propto 1/|x| \tag{12}$$

so that the relevant critical exponent is $\beta = 1$; it is different from the result for an impenetrable film, $\beta = 4/3$ [21]. (Note that the polymer actually forms two equivalent and connected adsorbed layers on both sides of the film). Equation (12) is valid for $\Delta \ll |x| \ll x_{max}$, where

$$x_{max} = x(L) \sim L^{3/2}/l^{1/2} \tag{13}$$

Equation (12) implies that most of polymer segments are far from the film (i.e., they belong to loops). The fraction p of segments in the Δ -layer is

$$p \sim c(\Delta)\Delta / \int_0^{x_{max}} c(x) dx \tag{14}$$

leading to $p \sim 1/\ln(N)$, where $N \equiv L/\lambda$. The total potential energy of critically adsorbed chain (at $u = u^*$) is

$$E = -uTLp \sim -TN/\ln N \tag{15}$$

and the number of polymer contacts with the film is $n_c \propto \tilde{N} \equiv N/\ln(N)$ which formally corresponds to $\phi = 1$ (cf. Equation (1)).

2.3. Dependencies of Energy, Free Energy and Concentration Profiles on the Attraction Strength u

In this section, we continue to consider the regime $\lambda \ll L \lesssim l$ for a chain with ends located in the Δ -layer. At $u = 0$, there is no polymer/film interactions, and the chain behaves as a single loop. In this case, the monomer concentration at $x \sim x(s)$ is $c_0(x) \sim s/x(s)$ leading to the power law: $c_0(x) \propto x^{-1/3}$ for $|x| \lesssim x_{max}$ at $u = 0$ (non-adsorbed state). By contrast, $c_1(x) \propto x^{-\beta}$ for $u = u^*$ (critically adsorbed state). In the

general case, for $u < u^*$, the concentration profile can be represented (with the scaling accuracy) by $c_1(x)$ for short x , $x < \Lambda$, and $c_0(x)$ for $x > \Lambda$ (cf. ref. [21]), leading to the following interpolation:

$$c(x) \propto (x/\Lambda)^{-1/3} + (x/\Lambda)^{-\beta}, \quad u < u^* \tag{16}$$

where Λ depends on the deviation τ from the critical point, $\tau \equiv u/u^* - 1$. At $\tau = 0$, the profile is self-similar (cf. Equation (12)), so the first term in Equation (16) can be neglected. It is important, however, that the critically adsorbed state (corresponding to the second term in Equation (16)) is highly sensitive to a variation of τ . Indeed,

$$\frac{\partial F}{\partial \tau} = -u^*TLp \sim -T\tilde{N} \text{ at } \tau = 0 \tag{17}$$

where F is the free energy of the adsorbed chain, E_Γ is the potential energy of a configuration Γ , $E_\Gamma = -uTLp_\Gamma$ (cf. Equation (15)), $\tilde{N} = N/\ln N$, and we used the theorem on small variations [28]:

$$\frac{\partial F}{\partial \tau} = \left\langle \frac{\partial E_\Gamma}{\partial \tau} \right\rangle = -u^*TL\langle p_\Gamma \rangle \tag{18}$$

Here $\langle \odot \rangle$ meaning the ensemble average of \odot over all configurations and $\langle p_\Gamma \rangle = p$. Therefore,

$$\Delta F \equiv F(\tau) - F(0) \simeq -T\tilde{N}\tau$$

for a small $|\tau|$, so that a small negative τ can significantly destabilize the self-similar state (cf. Equation (12)): for $\tau < 0$, $|\tau| \gg 1/\tilde{N}$, its free energy increases by $\Delta F \gg T$, and its statistical weight decreases by a large factor $e^{\Delta F/T} \gg 1$, leading to $\Lambda \ll x_{max}$ (cf. Equation (16)). On the other hand, at $|\tau| \sim 1/\tilde{N}$, the destabilization is marginal and $\Lambda \sim x_{max}$, i.e.,

$$\Lambda \sim x_{max} \sim N^{3/2}\Delta \text{ for } \tau = \tau^* = -\ln N/N$$

Assuming that Λ is a function of τ only (i.e., it is nearly independent of N) as long as $|\tau| \gtrsim 1/\tilde{N}$ (which is equivalent to $x_{max} \gtrsim \Lambda$) and neglecting the $\ln N$ factor, we find

$$\Lambda \sim \tau^{-3/2}\Delta, \quad |\tau| \gg 1/N, \quad \tau < 0 \tag{19}$$

The τ -dependence of the total energy is defined by equation $E = -u^*TL(1 + \tau)p$. Using Equations (16), (19) and (14), we thus obtain for $\tau < 0$, $1/N \ll |\tau| \ll 1$:

$$p \sim (|\tau|N)^{-1} \tag{20}$$

$$E \sim -T/|\tau| \tag{21}$$

The dependence of the chain free energy F on τ can be deduced from Equation (18):

$$\frac{\partial F}{\partial \tau} = -u^*TLp \tag{22}$$

(cf. Equation (17)). Using also Equation (20) we get for $\tau < 0$:

$$F(\tau) - F(0) \sim T \ln(|\tau|N), \quad 1/N \ll |\tau| \ll 1 \tag{23}$$

Note that for $u = 0$ ($\tau = -1$), the chain partition function is $Z_l(L) \propto \frac{1}{x(L)\theta(L)} \propto 1/N^2$, so

$$F(-1) \simeq 2T \ln N \tag{24}$$

suggesting (by virtue of Equation (23)) that $F(0) \sim T \ln N$. (Note that by virtue of Equations (14) and (16), the assumption adopted above Equation (19) is equivalent to assuming that the number of polymer/membrane contacts $n_c(\tau) \propto pN$ depends on τ but not

on the chain length at $\tau < 0$, $|\tau|n_c(0) \gg 1$. This is a standard assumption of the scaling theory of polymer adsorption [4]).

Let us turn to the regime of adsorbed chain, $u > u^*$, i.e., $\tau > 0$. The reduced adsorption energy per unit length,

$$\epsilon \simeq -F/(TL)$$

gets positive and significant in this regime (in contrast to the pre-adsorption regime, $\tau < 0$, where Equations (23) and (24) lead to $|\epsilon| \sim 1/L$). The dependence of ϵ on τ for $\tau > 0$ can be obtained using the general Equation (22):

$$\frac{\partial \epsilon}{\partial \tau} = u^* p \tag{25}$$

To obtain p using Equation (14), we need to know the concentration profile for $\tau > 0$. To this end, we can use the same argument as that proposed in Section 2.2 to obtain the self-similar profile at $\tau = 0$. The only difference is that for $\tau > 0$ (and hence, as verified below, $\epsilon > 0$) the partition function $Z_l(s)$ of a loop (with $s \gg \lambda$) must be replaced by a modified one:

$$Z_{l\epsilon}(s) = Z_l(s)e^{-\epsilon s} \propto s^{-2}e^{-\epsilon s} \tag{26}$$

where $Z_l(s)$ is defined in Equation (11). Here the statistical factor $e^{-\epsilon s} = e^{-\Delta F/T}$ accounts for the free energy penalty $\Delta F = T\epsilon s$ for the desorption of a large s -loop we consider. For $s < s^* = 1/\epsilon$, the new factor is not important, so the critical law, Equation (12), stays valid for $x \ll h$:

$$c(x) \propto x^{-1}, \quad x \ll h \tag{27}$$

where

$$h \equiv x(s^*) = l^{-1/2}\epsilon^{-3/2} \tag{28}$$

(here we also assume that $h \ll x_{max}$, that is $\epsilon L \gg 1$). Obviously, for $x > h$ ($s > s^*$), the loops are suppressed, so the concentration $c(x)$ decays exponentially. The decay law for $x \gg h$ was established in ref. [21]:

$$c(x) \propto \exp\left(-\frac{4}{3}\left(\frac{12x}{h}\right)^{1/2}\right), \quad x \gg h \tag{29}$$

It is clear that the region $x \gg h$ can be neglected in the integral of Equation (14), which gives

$$p \sim 1/\ln(h/\Delta) = -k_1/\ln(\epsilon\lambda) \tag{30}$$

where k_1 is a numerical factor. Equations (25) and (30) then give

$$\lambda \frac{d\epsilon}{d\tau} = -k_2/\ln(\epsilon\lambda)$$

where $k_2 = k_1 u^* \lambda$ is another numerical factor (cf. Equations (5) and (7)). The above equation leads to

$$\epsilon \simeq (k_2/\lambda)\tau/\ln(1/\tau), \quad 1 \gg \tau \gg 1/N \tag{31}$$

The obtained critical behavior of the free energy per unit length points to a second-order phase transition at $\tau = 0$. According to Equation (28), the thickness of the adsorbed layer, h , rapidly decreases with τ roughly as $h \propto \tau^{-3/2}$. By contrast, the fraction p of monomers in contact with the film (in the Δ -layer) increases logarithmically, $p \propto 1/\ln(1/\tau)$ for $1 \gg \tau \gg 1/N$.

3. Quantitative Approach

The scaling results described above can be also justified with a quantitative theory accounting for both spatial and orientational distributions of polymer segments. Following

ref. [21], let us consider a semirigid chain of length L with one free end and the second end having position x and orientation \underline{n} (cf. Figure 1b).

The partition function of such an ideal chain in the presence of the membrane potential ($U(x)$ at $|x| < \Delta$) is $\psi(x, \underline{n}, L)$. Its change as L grows can be described by the transfer-matrix approach, leading to the master equation (the generalized Edwards equation) [18,21,29,30]:

$$\frac{\partial \psi}{\partial L} = \frac{1}{l} \nabla_{\underline{n}}^2 \psi - n_x \frac{\partial \psi}{\partial x} - \frac{U(x)}{T} \psi \quad (32)$$

(note that ψ does not depend on the y, z coordinates in the membrane plane). At large L , the function ψ must tend to the ground state with

$$\psi(x, \underline{n}, L) \rightarrow e^{\epsilon L} \psi(x, \underline{n}),$$

where $\psi(x, \underline{n})$ is the ground eigenfunction (corresponding to the largest ϵ) of the operator on the rhs of Equation (32):

$$\frac{1}{l} \nabla_{\underline{n}}^2 \psi - n_x \frac{\partial \psi}{\partial x} - \frac{U(x)}{T} \psi = \epsilon \psi \quad (33)$$

A similar equation was derived in ref. [21]. Here

$$\epsilon \equiv \lim_{L \rightarrow \infty} (-F/(TL)) \quad (34)$$

where F is the chain free energy increment due to interactions with the membrane. Below, we focus on the layer structure at distances $|x| \ll l$ in the limit of long chains $L \gg l$. Taking into account that \underline{n} -dependence of ψ reduces to its dependence on the angle $\theta \simeq n_x$ between \underline{n} and the plane, and that $|\theta| \ll 1$ for $|x| \ll l$ (the condition $|\theta| \ll 1$ is suggested by the scaling analysis in Section 2.2), we rewrite Equation (33) as (in analogy with ref. [21])

$$\frac{1}{l} \frac{\partial^2 \psi}{\partial \theta^2} - \theta \frac{\partial \psi}{\partial x} - \frac{U(x)}{T} \psi = \epsilon \psi \quad (35)$$

where $\psi = \psi(x, \theta)$. This equation is obviously invariant with respect to substitutions $x \rightarrow -x, \theta \rightarrow -\theta$, implying an obvious symmetry

$$\psi(-x, -\theta) = \psi(x, \theta) \quad (36)$$

Furthermore, as the film is penetrable, we should demand that

$$\psi(-\Delta, \theta) = \psi(\Delta, \theta) \text{ for } \theta \gg \theta_{\Delta} \equiv (\Delta/l)^{1/3} \quad (37)$$

The above equation simply states that partition functions of chains with ends at A_- and A_+ (cf. Figure 2) are nearly equal. The condition $\theta \gg \theta_{\Delta}$ provides that (i) the potential energy due to the end segment (of length $s_{int} \simeq 2\Delta/\theta$) of chain A_+ penetrating the membrane is low (as compared to T), so that the potential energies of the two chains are nearly equal, and (ii) the bending of the s_{int} -segment is negligible compared to θ so that the end angles of both chains are nearly equal to θ (cf. Figure 2).

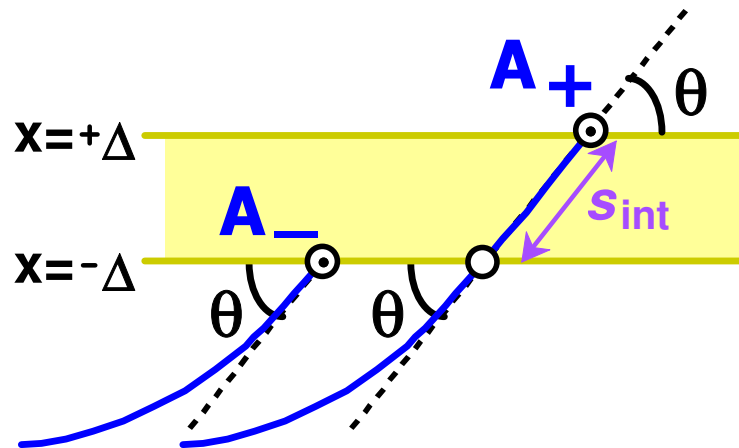


Figure 2. Two chains with the same orientation at $x = -\Delta$ defined by the angle $\theta > 0$. One chain ends at point A_- just below the membrane. The second chain ends at point A_+ slightly above the membrane intersecting it with the end segment of length s_{int} .

Our primary goal is to find $\psi(x, \theta)$ at the critical point $u = u^*$. As discussed in Section 2.3 at this point ϵ vanishes (actually, it nearly vanishes and can be neglected, see Section 4 below). It was also shown in Section 2.2 that the concentration profile at $u = u^*$ follows an algebraic law, Equation (12), for

$$l \gg |x| \gg \Delta \tag{38}$$

It is therefore reasonable to assume (again following ref. [21]) a self-similar x -dependence of ψ (in the regime of Equation (38)):

$$\psi(x, \theta) = x^\alpha f(\theta/\theta_x), \quad x > 0 \tag{39}$$

where α is a constant to be determined, and θ_x is a function of x . To obtain $\psi(x, \theta)$ for $x < 0$, one should use the symmetry relation, Equation (36). The dependence $\theta_x = (x/l)^{1/3}$ simply follows from the structure of Equations (35) and (39) with $\epsilon = 0$ and $U(x) = 0$ for $x > \Delta$; it was obtained in ref. [21]. As a result, we arrive at the following equation for $f(\eta)$ with $\eta \equiv \theta/\theta_x$ (cf. ref. [21]):

$$\frac{\partial^2 f}{\partial \eta^2} + \frac{1}{3} \eta^2 \frac{\partial f}{\partial \eta} - \alpha \eta f = 0 \tag{40}$$

(Note that η here has the opposite sign compared to ref. [21]). The boundary condition for $f(\eta)$ stemming from Equation (37) is:

$$f(-\eta) \simeq f(\eta) \quad \text{for } \eta \rightarrow \infty \tag{41}$$

It is crucially different from that adopted in ref. [21]. Following the approach of ref. [21], the differential Equation (40) can be reduced to the Kummer equation, and $f(\eta)$ can be expressed in terms of degenerate hypergeometric functions:

$$f(\eta) = \Psi(-\alpha, 2/3, -\eta^3/9) \tag{42}$$

which is selected by the condition that $f(\eta)$ must not increase exponentially at $|\eta| \rightarrow \infty$. Here

$$\Psi(a, b, z) = \Gamma \left[\begin{matrix} 1-b \\ a-b+1 \end{matrix} \right] F(a, b, z) + \Gamma \left[\begin{matrix} b-1 \\ a \end{matrix} \right] z^{1-b} F(a+1-b, 2-b, z) \tag{43}$$

is the Tricomi function, and $F(a, b, z)$ is the standard degenerate hypergeometric function (${}_1F_1$). For $-\eta \gg 1$ the function, Equation (42), shows a power law behavior:

$$f(\eta) \simeq 3^{2\alpha} (-\eta)^{-3\alpha} \tag{44}$$

The parameter α can be obtained based on the physical boundary condition, Equation (41), which leads to the following equation:

$$\sin\left(\frac{2\pi}{3}\right) + \sin(\pi\alpha) = \sin\left(\frac{2\pi}{3} + \pi\alpha\right) \tag{45}$$

It has two series of roots:

$$\alpha = 2n, \alpha = 2n - 2/3$$

with integer n . As we look for ground states, $f(\eta)$ must not have any knots at finite η . This condition selects just two values: $\alpha = \alpha_0 = 0$ and $\alpha = \alpha_1 = -2/3$. The corresponding eigenfunctions are

$$\psi_0(x, \theta) = 1, \psi_1(x, \theta) = x^{-2/3} \Psi(2/3, 2/3, -\theta^3 l / (9x)) \tag{46}$$

For $|\theta| \gg (x/l)^{1/3}$, we obtain (cf. Equation (44)) $\psi_1(x, \theta) \simeq \text{const } \theta^{-2}$. Obviously, ψ_0 reflects an isotropic state at $u = 0$, while ψ_1 describes the strongly anisotropic critically adsorbed state at $u = u^*$. In other words, ψ_0 corresponds to the trivial isotropic adsorption point ($u = 0$) which is characteristic for both ideal flexible and long semiflexible chains (see the next section for a further discussion).

The monomer density distribution in the (x, θ) space is [21,30,31]

$$c(x, \theta) = \text{const } \psi(x, \theta) \psi(x, -\theta) \tag{47}$$

Therefore, $c_0(x, \theta) = \text{const}$, i.e., the chain stays free in the pre-adsorbed state ($u = 0$), its monomers are distributed uniformly and isotropically. By contrast, the distribution $c_1(x, \theta)$ in the critical state for strong adsorption (corresponding to $u = u^*$, $\alpha = \alpha_1$) is highly anisotropic and x -dependent:

$$c_1(x, \theta) = C_1 (x/l)^{-4/3} \rho(\theta/\theta_x) \tag{48}$$

where $C_1 = \text{const}$ and

$$\rho(\eta) = C_N \Psi(2/3, 2/3, -\eta^3/9) \Psi(2/3, 2/3, \eta^3/9) \tag{49}$$

Here, $C_N \approx 0.044175$ is the normalization constant defined by the condition

$$\int \rho(\eta) d\eta = 1 \tag{50}$$

The universal function $\rho(\eta)$ defines the orientational distribution of all polymer segments at a distance x ($\Delta \ll x \ll l$) from a penetrable membrane. This function is plotted in Figure 3.

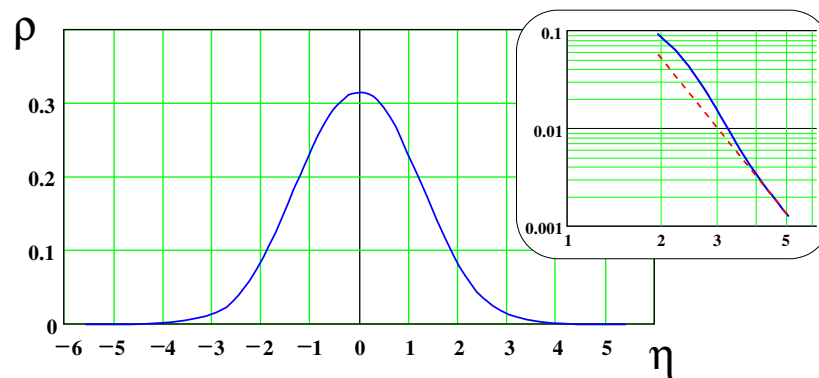


Figure 3. The normalized distribution (see Equation (49)) of the reduced angle $\eta = \theta(l/x)^{1/3}$ in the proximal aligned layer, where θ is the angle of a chain segment and x is its distance to the membrane. Inset: The same function in the log-log scale. The dashed line indicates the asymptotic law, $\rho \propto \eta^{-4}$ for $|\eta| \gg 1$ (cf. Equation (51)).

Note that $\rho(\eta)$ shows a power-law decay, $\rho \propto \eta^{-4}$, at large η ($|\eta| \gg 1$) as demonstrated in the inset of Figure 3. This is in contrast to a very strong compressed exponential decay predicted in ref. [21] for the case of adsorption to an impenetrable solid surface. Interestingly, for $|\theta| \gg \theta_x$, the $c_1(x, \theta)$ distribution depends on the angle θ , but is almost independent of x

$$c_1(x, \theta) = \text{const } \theta^{-4}, \quad |\theta| \gg \theta_x \tag{51}$$

The reason for this behavior is simple: the relevant chain segments of length x/θ can be considered straight.

The monomer density as a function of distance only is $c(x) = \int c(x, \theta)d\theta$ (here the integration limits are $-\pi/2$ and $\pi/2$, but note that for $x \ll l$ the integral mainly comes from $|\theta| \sim \theta_x \ll 1$). At the adsorption threshold, we obtain $c_1(x) \propto x^{-1}$ for $x \ll l$ in agreement with the scaling result, Equation (12).

4. Dependence of the Adsorbed Layer Structure on the Attraction Strength

In the previous section, we rederived the critical exponent for the self-similar concentration profile at $u = u^*$ using the transfer-matrix theory. We are now in a position to consider the dependence of the adsorption profile on $\tau = u/u^* - 1$. At this point, it is important to note that, strictly speaking, $u = u^*$ does not correspond to the chain-trapping transition: a purely attractive potential $U(x)$ we consider always traps a long ($L \rightarrow \infty$) chain for whichever low attraction strength u . This statement is well-known for flexible chains [4], and it is also valid for wormlike chains, which behave as flexibly at length scales $\gg l$ [21]. To show this, let us consider a long ideal wormlike chain ($L \gg l$) near an attractive penetrable membrane with $0 < u < u^*$. Assuming that the chain conformation is unperturbed by the potential, one can easily estimate the total potential energy of such a chain:

$$E \sim -uTL\Delta/R \sim -uT\Delta\sqrt{L/l}$$

where R is the chain size defined in Equation (3). The chain is trapped by the membrane if $|E| \gg T$, i.e., for

$$u \gg \Delta^{-1}\sqrt{l/L}$$

Hence, for $L \rightarrow \infty$, the chain is indeed trapped for any $u > 0$. This conclusion stays valid also if a perturbation of the chain conformation by the membrane potential is taken into account since such a perturbation must always increase $|E|$.

Then the natural question arises: what is the meaning of u^* if the adsorption occurs already at $u = 0^+$? The answer is that u^* defines the second transition to a strongly anisotropic adsorbed state accompanied by the formation of a self-similar layer. This point and the features of both transitions are further discussed below.

The argument given above shows that the reduced adsorption energy per unit length, ϵ , is always positive for $u > 0$. Let us consider the distal region, $x \gg l$, of the adsorbed layer. Here we can apply the classical equation (cf. ref. [32] and Equation (25) of ref. [21]) for an ideal flexible chain:

$$\frac{l}{6} \frac{\partial^2 \psi}{\partial x^2} = \epsilon \psi \tag{52}$$

where $\psi = \psi(x)$ is the partition function of the chain with one end at x , and $\epsilon > 0$ is considered as known parameter. The solution to the above equation for the concentration profile $c(x) \propto \psi(x)^2$ is

$$c(x) \simeq c_0 \exp(-|x|/h) \tag{53}$$

where

$$h = \frac{1}{2\sqrt{6}} \sqrt{l/\epsilon} \tag{54}$$

is the distal layer thickness. To find h , we eventually need to establish the dependence of $\epsilon = \epsilon(\tau)$ on the attraction strength. To this end, we have to obtain the whole concentration profile $c(x)$, and, in particular, its proximal part near the membrane, at $x \lesssim l$. At $u \ll u^*$, nothing special happens with $c(x)$ in this proximal region: Equation (53) remains valid there, and the same is true for $u \sim u^*/2$. To see this, recall that the interaction energy of an l -segment intersecting the membrane at an angle θ is $E_{int} \simeq -2uT\Delta/\sin\theta = -E_1/\sin\theta$ (cf. Figure 2), where $E_1/T = 2u\Delta \lesssim u^*\Delta \sim (\Delta/l)^{1/3} \ll 1$. Therefore, for most θ , the interaction energy is small ($|E_{int}| \ll T$); hence, the segment positional and orientational distribution is only slightly perturbed by the membrane potential. It remains nearly uniform and isotropic at $x \lesssim l$ in accordance with Equation (53). It is only at the lowest possible angles, $\theta \sim \theta_\Delta \ll 1$ (cf. Equation (37)), that the perturbation is moderate ($|E_{int}| \sim T$), so that tangential orientations (with low θ) are somewhat preferred. Still the overall orientational order parameter $S_{or} = 0.5\langle 3\sin^2\theta - 1 \rangle$ remains small: $|S_{or}| \sim \theta_\Delta \sim (\Delta/l)^{1/3} \ll 1$ (a logarithmic factor is neglected here).

The situation changes only at $u \approx u^*$ ($|\tau| \ll 1$), where ‘trains’ (sequences of tangentially oriented segments) and loops start to form near the membrane. At $u = u^*$ ($\tau = 0$), they result in a self-similar concentration profile, $c(x) \propto 1/|x|$, and strong ‘disklike’ orientation of polymer segments, $S_{or} \simeq -0.5$, in the proximal layer at $|x| \ll l$ (cf. Sections 2.2 and 3). This structure is due to a fractal distribution of polymer loops. At a weaker attraction, $u < u^*$ ($\tau < 0$), the self-similar region becomes thinner. To quantify this effect, let us firstly recall that the fractal structure of loops emerges at $u = u^*$ because in this case, a detachment of a ‘train’ (its conversion into a loop) never costs any significant free energy: the entropic free energy due to the ‘train’ confinement in the Δ -layer is exactly compensated by the negative energy gain due to the membrane potential. This balance is broken at $\tau < 0$ when the potential energy gain is decreased. As a result, a conversion of a ‘train’ of length $s = g\lambda$ into a loop now leads to an additional negative free energy $\Delta F = (u - u^*)sT \sim \tau gT$, $\tau < 0$ (cf. Equations (5) and (7)). Its effect can be neglected for $g \lesssim g^* \sim 1/|\tau|$ (i.e., $s \ll s^* \sim \lambda/|\tau|$), but it destroys the self-similar structure at larger s . The thickness Λ of the fractal layer at $\tau < 0$ is, therefore, defined by the x -size of the crossover loops of length $\sim s^*$:

$$\Lambda \sim \Delta/|\tau|^{3/2}, \quad \tau < 0, \quad |\tau| \gtrsim \lambda/l \tag{55}$$

Note that the above equation agrees with Equation (19). The condition $|\tau| \gtrsim \lambda/l$ reflects the fact that the maximal thickness of the self-similar layer is $\sim l$; hence $\Lambda \sim l$ for $|\tau| \lesssim \lambda/l \sim (\Delta/l)^{2/3}$. The whole adsorbed layer (at $x > 0$) is shown schematically in Figure 4.

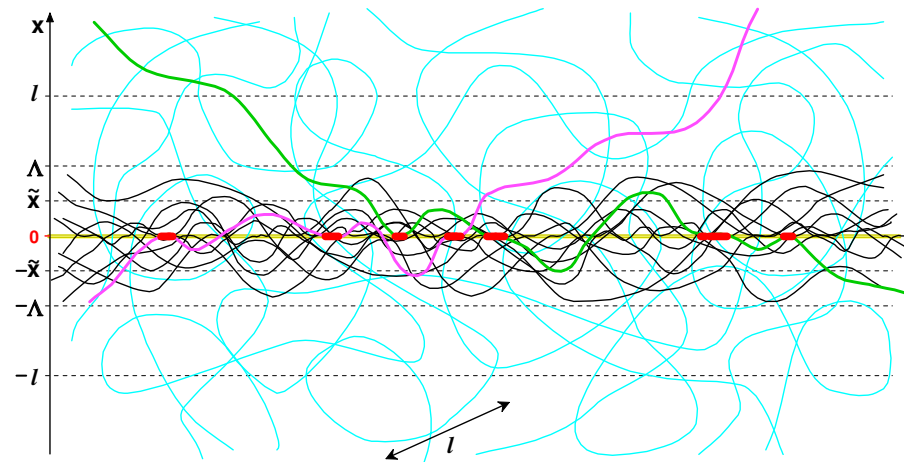


Figure 4. The structure of loops formed by a wormlike chain near a penetrable membrane at a near-critical adsorption strength, $u \approx u^*$, $u < u^*$. There are long semiflexible isotropic loops (shown in cyan) everywhere, while shorter aligned loops (shown in black) are present only close enough to the membrane. Aligned loops show a fractal distribution for $|x| \lesssim \Lambda$, and they dominate by mass in the proximal layer at $|x| \lesssim \tilde{x}$, where $\tilde{x} < \Lambda$. The aligned loops virtually merge with long isotropic loops at the crossover distance $|x| \sim \Lambda$ (see green and pink fragments as examples).

Thus, the self-similar structure of loops is predicted in the proximal sublayer, $\Delta < x < \Lambda$. At the crossover, $x \sim \Lambda$, the proximal loops (of length $s \lesssim s^*$) readily conjugate with nearly isotropic larger loops of size $\gtrsim l$, which dominate further away from the membrane. The conjugation means that concentration $c_{ll}(x, \theta)$ of due to large loops and $c_{ss}(x, \theta)$ due to self-similar loops (of size $s \sim s^*$) must be comparable at $x = \Lambda$ and $\theta \sim \theta_\Lambda \sim (\Lambda/l)^{1/3}$ (recall that proximal loops are mostly oriented tangentially to the surface, cf. Equation (39)). Obviously $c_{ll}(x, \theta) \sim c_0$ (cf. Equation (53)). As for $c_{ss}(x, \theta)$, it is given in Equation (48): $c_{ss}(x, \theta) \sim C_1 (x/l)^{-4/3}$ for $\theta \lesssim \theta_x$. The conjugation condition therefore gives $C_1 \sim c_0(\Lambda/l)^{4/3}$ so that the total concentration $c \simeq c_{ll} + c_{ss}$ is

$$c(x, \theta) \sim c_0 \left[1 + (x/\Lambda)^{-4/3} \rho(\theta/\theta_x) \right], \quad \Delta < x \lesssim l \tag{56}$$

The total concentration profile obtained by integration over θ therefore is (note that $c_{ss}(x) = \int c_{ss}(x, \theta) d\theta \sim C_1 l/x$)

$$c(x) \simeq c_0 \left[1 + \frac{\tilde{x}}{x} \right], \quad \Delta < x \lesssim l \tag{57}$$

where

$$\tilde{x} \sim \frac{\Lambda^{4/3}}{l^{1/3}} \tag{58}$$

(Note that by continuity $c(x) \sim c_0(1 + \tilde{x}/\Delta)$ for $|x| < \Delta$). The whole concentration profile at $x > \Delta$ is defined by Equations (53) and (57). The whole adsorbed layer can be viewed as a superposition of ‘trains’ at $|x| \sim \Delta$, aligned self-similar loops and nearly isotropic longer fragments of size $\gtrsim l$. The aligned loops disappear for $\tau < 0$, $|\tau| \sim 1$: in this case $\Lambda \sim \Delta$, so the loops are short and can be considered as parts of ‘trains’. Furthermore, the contribution of both aligned loops and trapped ‘trains’ can be neglected in the total concentration $c(x)$ if $|\tau| \gtrsim (\Delta/l)^{1/6}$ (corresponding to $\tilde{x} \lesssim \Delta$, cf. Equations (58) and (55)).

We are now in a position to obtain the dependence of ϵ and h on τ . To this end, we use the general Equation (25): $\frac{\partial \epsilon}{\partial \tau} = u^* p \sim p/\lambda$, where p is the fraction of trapped monomers (cf. Equation (14))

$$p = \frac{\int_0^\Delta c(x) dx}{\int_0^\infty c(x) dx} \tag{59}$$

Using $c(x)$ defined above and Equations (55) and (58), we obtain (generally neglecting log-factors)

$$p \sim \frac{\Delta + \tilde{x}}{h},$$

$$\tilde{x} \sim \begin{cases} \frac{\Delta^{4/3}}{l^{1/3}} |\tau|^{-2}, & (\Delta/l)^{1/6} \gtrsim |\tau| \gtrsim (\Delta/l)^{2/3} \\ l, & |\tau| \lesssim (\Delta/l)^{2/3} \end{cases}$$

Solving Equation (25) with initial condition, $\epsilon = 0$ for $u/u^* = 1 + \tau = 0$, we obtain for $\tau < 0$:

$$\epsilon l \sim \begin{cases} \delta^2(1 + \tau)^2, & |\tau| \gtrsim \delta \\ |\tau|^{-2} \delta^4, & \delta \gtrsim |\tau| \gtrsim \delta^2 \\ 1, & |\tau| \lesssim \delta^2 \end{cases} \quad (60)$$

where $\delta \equiv (\Delta/l)^{1/3}$. Note that $\epsilon L \gtrsim 1$ is required for adsorption and that for $u \ll u^*$ Equation (60) gives $\epsilon L \sim (L/l)\delta^2(u/u^*)^2$. The latter equation shows that $\epsilon L \ll 1$ and, hence, the chain is not adsorbed (and not really affected by attraction to the membrane) for $L \lesssim l/\delta^2 = L_m$ in agreement with Equation (9). By contrast, for $L \gg L_m$ and $u \sim u^*/2$, the chain must be well-adsorbed (trapped by the membrane), but the proximal anisotropic layer is not yet formed since for $\tau \equiv u/u^* - 1 \sim -1/2$ the crossover distance $\Lambda \sim \Delta$ and $c(x)$ is always dominated by the isotropic contribution of long semiflexible loops.

The terminal thickness h of the adsorbed layer (cf. Equation (54)) for $\tau < 0$ therefore is

$$h \sim \begin{cases} l\delta^{-1}(1 + \tau)^{-1} = l^{4/3}\Delta^{-1/3}u^*/u, & |\tau| \gtrsim \delta \\ l|\tau|/\delta^2, & \delta \gtrsim |\tau| \gtrsim \delta^2 \\ l, & |\tau| \lesssim \delta^2 \end{cases} \quad (61)$$

Thus all the 3 length-scales, h , Λ and \tilde{x} becomes similar to the Kuhn segment l near the critical point $u = u^*$ ($|\tau| \lesssim \delta^2$) for the second (anisotropic) adsorption transition. At this point $\epsilon \sim 1/l$, so the effect of ϵ can be neglected in the proximal anisotropic layer of relatively short aligned loops (whose length $s \ll l$).

Above u^* (at $\tau > 0$), the adsorbed layer structure is characterized by a single length-scale h (apart from the ‘nano-scale’ Δ). The concentration profile, ϵ and h can be obtained in exactly the same way as discussed in Section 2.3 (cf. Equations (27), (29) and (31)):

$$c(x) \sim \text{const } x^{-1} \exp\left(-\frac{4}{3}\left(\frac{12x}{h}\right)^{1/2}\right), \quad x \gg \Delta$$

$$\epsilon l \sim \begin{cases} 1, & 0 < \tau \lesssim \delta^2 \\ \delta^{-2}\tau/\ln(1/\tau), & 1 \gtrsim \tau \gg \delta^2 \end{cases} \quad (62)$$

$$h \simeq l/(\epsilon l)^{3/2} \sim \begin{cases} l, & 0 < \tau \lesssim \delta^2 \\ \Delta[\ln(1/\tau)/\tau]^{3/2}, & 1 \gtrsim \tau \gg \delta^2 \end{cases} \quad (63)$$

The layer thickness h therefore decreases with τ ; it changes from $h \sim l$ at $\tau = 0$ to $h \sim \Delta$ at $\tau \sim 1$.

5. Preliminary Discussion

In the previous sections, we considered the adsorption of wormlike polymers to a flat penetrable membrane. Modeling a membrane (a free-standing film) as just a potential energy profile, which is uniform along the membrane plane (cf. Equation (4)), may seem to be far from reality. However, in the spirit of a mean-field approach, it is really plausible to represent a film by an effective potential of its interaction with the adsorbed macromolecule. The mean molecular potential can reflect the film structure in the normal direction (across the film). On the other hand, the heterogeneous film structure in the lateral direction can be

neglected if the corresponding correlation length is smaller than the characteristic lateral size λ associated with the wormlike polymer (cf. Equation (7)).

Nevertheless, it would be useful to consider some specific physical realizations of penetrable membranes. It is well-known that many polymers tend to adsorb to surfactant layers, including free-standing double-layer surfactant vesicles and lipid bilayers [33]. Interfaces between surfactant layers and polymers are known to be highly relevant to biophysical membrane problems [34]. In particular, the adsorption of semiflexible polymers at the exterior side of a membrane can induce changes of a vesicle or a biological cell shape [8]. Interactions of macromolecules with cell membranes are important for many processes in cell biology [8,10,11,35,36] including DNA uptake by cells. Biopolymers such as DNA normally use appropriate pores to penetrate cell membranes [37,38]. Importantly, it was recently established that a direct penetration across the cell membrane is possible for amphipathic phospholipid polymers mimicking the chemical structure of phospholipids in the membrane [9]. It is therefore reasonable to expect that a surfactant (lipid) bilayer in a disordered liquid state can be penetrable by a locally stiff macromolecule if it has some affinity to non-polar hydrophobic molecular fragments (tails) inside the bilayer. The macromolecule must be therefore amphiphilic with alternating polar/charged groups (to ensure aqueous solubility) and hydrophobic fragments. On the other hand, the macromolecular adsorption can be due to electrostatic attraction of ionic groups to oppositely charged 'heads' of surfactants in the bilayer membrane. A high salinity of the solution can be used to keep the electrostatic interactions sufficiently short-range so that the simple model of Equation (4) may be applicable in this case.

One should bear in mind, however, that the very penetration of a polymer end into the bilayer may imply a transient increase in the total free energy due to a disruption of the layer structure in a correlation volume near the penetration location. The penetration would then require to overcome an activation energy barrier. This feature is totally irrelevant for the equilibrium microstructure of the adsorbed polymer layers considered in this paper, but it may significantly slow down the layer formation and equilibration.

Instead of a free-standing surfactant layer, one can consider adsorption onto a simple interface between two immiscible solvents, such as water and a hydrophobic oily liquid. Here, the role of an adsorbing macromolecule can be taken by a weakly charged polyelectrolyte with a stiff (semiflexible) backbone. (Recall that most semiflexible biopolymers, such as double-strand DNA or F-actin, are charged). Such polyelectrolyte molecules can be soluble in both phases (in water, due to charged groups, and in oil, due to a hydrophobic backbone). The driving force for adsorption of such wormlike polymers at the interface can be provided by their amphiphilic nature: both types of polymer groups can benefit from a favorable environment near the interface, for example, if the charged groups are grafted to the hydrophobic backbone with flexible spacers. The general problem here is that the polymer, being soluble in both phases, may still prefer one of them. It can be possible, however, to restore the symmetry (to render the solvation free energies in both solvents equal) by tuning the ion strength (or pH) in the water phase.

Yet another possibility is to consider an ultra-thin solid film with nano-holes in it. For the theoretical approach developed in this paper to be applicable, the nano-holes (of diameter D) must be much larger than the film attraction range Δ , but much smaller than the polymer rigidity segment l : $\Delta \ll D \ll l$ (in addition, $D\theta_\Delta$ must be larger than the chain thickness d). A polymer adsorption layer can be then naturally formed due to polymer/film attraction, while, in addition, the semiflexible polymer fragments can easily penetrate the layer through the holes. Modern technologies offer a number of techniques to create such porous ultra-thin membranes [39–44]. In particular, 1 nm thick carbon nano-membranes with pores of diameter 3–30 nm were produced [45].

In the next section, we show that complexes of wormlike polymers with such porous membranes show some universal features, which require a special analysis provided there.

6. Partially Penetrable Membranes

Let us consider an ultra-thin solid nanolayer (for example, a free-standing carbon, metal or polymer nanosheet) of effective thickness 2Δ (including its attraction zone, see Figure 5) perforated with nano-holes of diameter $\sim D$. The regime of interest is $\Delta \ll D \ll l$. We keep considering a very long semiflexible chain, $L \gg l$. The polymer fragments can penetrate the layer through the holes. Otherwise, the adsorbed fragments can stay near the solid surface, while polymer penetration inside the solid film is not allowed (cf. Figure 5). The membrane attraction potential is defined, as before, in Equation (4), where x should be now replaced by the distance to the solid surface (so, of course, the potential is virtually absent in the hole regions). The important parameter is the area fraction w of holes. The mean total area per hole is $\sim D^2/w$. The mean distance between the centers of neighboring holes is therefore $\sim D/\sqrt{w}$. To simplify the argument, we also assume that this distance exceeds the microscopic length λ along the membrane, $D/\sqrt{w} \gtrsim \lambda$.

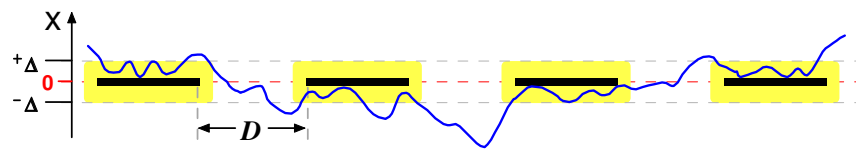


Figure 5. A wormlike chain near a porous solid nanofilm of effective thickness 2Δ . The chain can freely pass from one side of the film to the other through the holes of diameter $\sim D$.

At the adsorption threshold, $u = u^*$, the polymer creates a structure of loops. By a loop, here we mean a chain fragment whose both ends are located near the membrane surface (in the Δ -layer next to it) and are oriented nearly parallel to it. Such a loop can intersect the $x = 0$ plane. Let us focus on the loops with length s in the range $D/\sqrt{w} \ll s \ll l$. It corresponds to the following range of x -coordinates: $x_{min} \ll |x| \ll l$, where $x_{min} = x(D/\sqrt{w}) = D^{3/2}/(l^{1/2}w^{3/4})$ (cf. Equation (6)). It must be expected that a self-similar structure of loops is formed in this regime since the heterogeneous structure of the film becomes effectively coarse-grained at $|x| \gg x(D/\sqrt{w})$. As a result, each intersection of the nanolayer by the chain now brings an additional statistical weight factor w in the partition function (note that w is just the probability that the chain ‘finds’ a hole). Thus, the only difference with the reference model (Section 2) is related to the free energy cost of an intersection. Before (in Sections 2–4), it was equal to $E_{int} = -2uT\Delta/\sin\theta_{cross}$, now it is $-T \ln w$ independent of the crossing angle θ_{cross} .

Let us turn to the structure of loops for the membrane with holes. To start with, we switch off any interactions with the membrane (located around the $x = 0$ plane). Let $Z_l(s|n)$ denote the partition function of a loop of contour length s involving n intersections with the plane, $x = 0$. The function $Z_l(s|0)$ for $n = 0$ was considered in ref. [21] (and denoted as $Z_l(s)$ there):

$$Z_l(s|0) \sim (s/\lambda)^{-5/2}, \quad s \lesssim l$$

On the other hand, the total partition function of a loop (with arbitrary number of intersections) for a perfectly permeable adsorbing film is

$$Z_l(s) = \sum_n Z_l(s|n) \tag{64}$$

As was established in Section 2.2 (Equation (11))

$$Z_l(s) \sim (s/\lambda)^{-2} \tag{65}$$

Therefore, the probability $p(s|0)$ that a loop has no crossings is

$$p(s|0) \equiv Z_l(s|0)/Z_l(s) \sim (s/\lambda)^{-0.5} \tag{66}$$

It is not difficult to estimate the *mean* number of intersections of a loop of length S , $\bar{n}(S)$. With the same scaling accuracy (i.e., omitting the numerical prefactor), the result is

$$\bar{n}(S) \simeq \text{const} \ln(S/\lambda) \tag{67}$$

The prefactor in the above equation can be obtained directly using the obvious relation $\bar{n}(S) \simeq 2 \int_{\lambda}^{S/2} P(s) ds$, where $P(s) ds$ is the probability that a chain element $(s, s + ds)$ intersects the $x = 0$ plane (s is the contour length from the nearest end of the loop). Obviously $P(s) ds \simeq \langle |\theta(s)| \delta(x(s)) \rangle ds \sim \langle |\theta(s)| \rangle ds / \langle |x(s)| \rangle$, where $\theta(s)$ is the tilt angle and $x(s)$ is the x -coordinate of the point s of the loop (recall that the typical $\theta(s) \sim (s/\lambda)^{0.5}$ and $x(s) \sim s\theta$, cf. Equation (6)). Taking into account the nearly Gaussian statistics of x and θ (at a given $s \ll l$), we obtain $P(s) \simeq \frac{\sqrt{3}}{2\pi} \frac{1}{s}$, so

$$\bar{n}(S) \simeq \frac{\sqrt{3}}{\pi} \ln(S/\lambda) \tag{68}$$

Equations (66) and (68) show that $p(s|0) \sim \exp(-\text{const} \bar{n})$ hinting at a Poisson-like distribution of n :

$$p(s|n) \equiv Z_l(s|n) / Z_l(s) \simeq (s/\lambda)^{-0.5} A^n / n! \tag{69}$$

with $A \sim \bar{n}(s)$. Below, we derive the above heuristic Equation (69) in a rigorous way, clarifying its approximate nature and its region of validity ($n \ll A^{2/3}$). A more precise value of A is also obtained (cf. Equations (79) and (80)).

Let us turn to a more general case with penalized intersections (defined by the factor w) corresponding to the adsorption on a semi-permeable plane (i.e., a membrane with holes). In the general case (arbitrary w), the definition of $Z_l(s)$, Equation (64), must be amended to take into account that n crossings bring the statistical weight w^n :

$$Z_l(s, w) = \sum_n Z_l(s|n) w^n \tag{70}$$

where we explicitly show for clarity that $Z_l(s, w)$ depends also on the penetration parameter w . (Note that defining $Z_l(s|n)$ in this section, we do not apply any restriction on the angle θ_{cross} between the membrane plane and a polymer fragment intersecting it: the reason is that intersections only occur in the hole regions where the surface potential is absent).

The problem to find $Z_l(s, w)$ can be treated alternatively using the master Equation (35) (see Section 3). Using the same substitution as before ($\psi(x, \theta) = x^\alpha f(\eta)$, $\eta = (l/x)^{1/3} \theta$ for $x > 0$; note that ψ for $x < 0$ comes from the general relation (36) due to the obvious symmetry of the problem) we obtain $\frac{1}{\eta} f'' + \frac{1}{3} \eta f' - \alpha f = 0$, which is equivalent to Equation (40).

Recalling that $\psi(x, \theta)$ is the partition function of a chain with the second end oriented at an angle θ to the plane and located at a distance $|x|$ from it, and comparing $\psi(0^+, \theta)$ and $\psi(0^-, \theta)$ for $\theta > 0$, we see that the only difference between $\psi(0^+, \theta)$ and $\psi(0^-, \theta) = \psi(0^+, -\theta)$ is that $\psi(0^+, \theta)$ involves one extra intersection near the end (cf. Figure 6). Hence

$$\psi(0^+, \theta) = w \psi(0^-, \theta) = w \psi(0^+, -\theta), \theta > 0 \tag{71}$$

where we also used Equation (36). (Note that physically 0^+ corresponds to $x = +\Delta$, 0^- to $x = -\Delta$, and the condition $\theta > 0$ should be replaced with $x \gg \theta_\Delta$. Equation (71) is applicable as a boundary condition since we are interested in $\psi(x, \theta)$ at relatively large length-scales, $|x| \gg \Delta$). Obviously, for $w = 0$, we return to the impenetrable wall problem considered in ref. [21], while $w = 1$ corresponds to the case of a perfectly permeable surface (cf. Section 3). In the general case, the condition (71) can be rewritten in terms of the function $f(\eta)$ as (cf. Equation (41)):

$$\lim_{\eta \rightarrow +\infty} \frac{f(\eta)}{f(-\eta)} = w \tag{72}$$

The solution of Equation (40) is

$$f(\eta) = \Psi(-\alpha, 2/3, -\eta^3/9)$$

where $\psi(a, b, z)$ is the Tricomi function (cf. Equation (42)) defined in Section 3. Using Equation (43) and other general properties of Ψ , we obtain the following equation defining α based on Equation (72):

$$\sin(\pi(2/3 + \alpha)) - \sin(\pi\alpha) = w \sin(2\pi/3)$$

It has two physically acceptable solutions (corresponding to a ground-state $f(\eta)$ without knots at finite η):

$$\alpha_0 = \frac{1}{6} - \frac{1}{\pi} \arcsin \frac{w}{2}, \quad \alpha_1 = -\frac{5}{6} + \frac{1}{\pi} \arcsin \frac{w}{2} \tag{73}$$

It is $\alpha = \alpha_1$ that corresponds to the critically adsorbed state (while α_0 describes the non-adsorbed case corresponding to $u = 0$, i.e., a sterically repulsive membrane with no attraction).

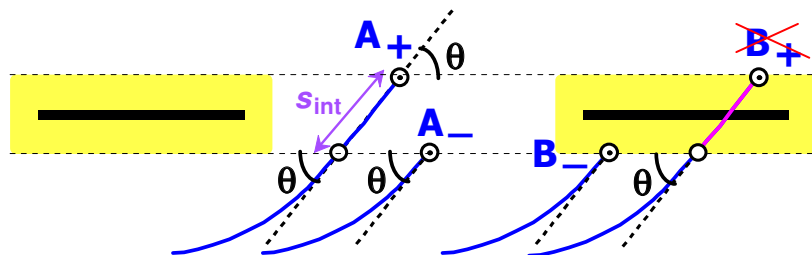


Figure 6. Clarification on Equation (71): The chain ending at point A_+ above the membrane intersects it through a hole. Otherwise, the conformation of this chain is similar to that of the chain A_- which ends below the membrane thus avoiding the last intersection. In analogy with Figure 2 the partition functions (ψ) of the chains A_- and A_+ are nearly equal, and the same is true, of course, for the chains A_- and B_- . By contrast, the partition function of the chain B_+ is zero since intersections of a solid part of the membrane are not allowed. On averaging over the film area, these relations lead to Equation (71).

The adsorbed layer can be considered as a system of loops. The number of loops of size s (per unit area) is proportional to $Z_l(s, w)$ so that the total length of monomers in all loops of size s , $S/2 < s < S$ is

$$L(S) \propto \int_{S/2}^S Z_l(s, w) s ds \sim S^2 Z_l(S, w)$$

Most of these monomers are located at a distance $\sim x(S) \sim S^{3/2}/l^{1/2}$ leading to concentration

$$c(x) \sim L(S)/x(S) \propto S^{1/2} Z_l(S, w) \text{ at } x \sim x(S) \tag{74}$$

Alternatively, the concentration profile can be obtained using the partition function $\psi(x, \theta)$ (cf. Equation (47)):

$$c(x) = \text{const} \int \psi(x, \theta) \psi(x, -\theta) d\theta = \text{const} |x|^{2\alpha+1/3} \int f(\eta) f(-\eta) d\eta$$

The second integral in the above equation converges to a numerical factor if $\alpha < -1/6$. The latter condition is always valid for $\alpha = \alpha_1$. Thus

$$c(x) \propto |x|^{2\alpha_1+1/3} \tag{75}$$

at the adsorption threshold. Thus, once again we arrive at a self-similar concentration profile, $c(x) \propto |x|^{-\beta}$ in the proximal layer $\Delta \lesssim |x| \lesssim l$ (cf. Equation (12) and ref. [21]), but now the critical exponent β depends on the membrane parameter w .

Comparing Equations (74) and (75) we finally obtain

$$Z_l(s, w) \sim (s/\lambda)^{3\alpha_1} \tag{76}$$

Obviously, for $w = 1$, the above equation agrees with Equation (65), while for $w = 0$, it agrees with the results of ref. [21] ($Z_l \propto s^{-5/2}$). Using Equations (76), (73) and (70) we obtain

$$\sum_n Z_l(s|n)w^n = \text{const} (s/\lambda)^{-5/2} (s/\lambda)^{(3/\pi) \arcsin(w/2)} \tag{77}$$

Therefore, the statistical weights of loops with n intersections, $Z_l(s|n)$ can be obtained by just performing Taylor expansion in w of the rhs of the above equation. Moreover, this equation allows to easily obtain all the moments of the distribution $p(s|n) = Z_l(s|n)/Z_l(s, 1)$. For example, the mean number of intersections is

$$\bar{n} = \partial \ln Z_l(s, w) / \partial \ln w = \frac{3}{\pi} \ln(s/\lambda) \frac{\partial}{\partial w} (\arcsin(w/2))$$

For $w = 1$, we thus obtain $\bar{n} = \frac{\sqrt{3}}{\pi} \ln(s/\lambda)$ in agreement with Equation (68). Using Equation (77), we find

$$\sum_n p(s|n)w^n \simeq (s/\lambda)^{-0.5} e^{2A \arcsin(w/2)} \tag{78}$$

with

$$A = \frac{3}{2\pi} \ln(s/\lambda) \gg 1 \tag{79}$$

For a small $w \lesssim 1/A$ the sum in the lhs of Equation (78) (which defines the generating function of the probability distribution) is dominated by a few terms with $n \sim 1$. Therefore, to obtain $p(s|n)$ for not too large n , we can assume $w \sim 1/A \ll 1$ and approximate $\arcsin(w/2)$ as $w/2$ yielding

$$\sum_n p(s|n)w^n \simeq (s/\lambda)^{-0.5} e^{Aw} \tag{80}$$

The above equation leads to the $p(s|n)$ distribution announced in Equation (69). A simple analysis shows that higher-order terms in the expansion of the arcsin in Equation (78) can be indeed neglected if $n \ll A^{2/3}$. Note that the Poissonian character of the n -distribution is not self-evident since crossings of chain fragments with the plane are strongly correlated.

7. Discussion

7.1. Discussion on Two Models of Polymer/Membrane Interactions

In this paper, we consider the reversible adsorption of a wormlike polymer to an ultra-thin penetrable free-standing membrane focusing on the equilibrium structure of the adsorbed polymer layer. The adsorption is driven by a short-range attraction between the membrane surface and polymer segments. Two basic models of the membrane are considered: (i) a perfectly penetrable amphiphilic fluid layer (a surfactant bilayer) whose effect can be accounted for by a short-range membrane potential, Equation (4); and (ii) a partially permeable porous nanofilm (solid membrane with nano-holes), cf. Sections 5 and 6. We found that in both cases, a strongly adsorbed anisotropic polymer layer (whose thickness is smaller than the Kuhn segment length l) is formed near the membrane slightly above the critical attraction strength u^* . In this regime, the number n_c of polymer/membrane contacts is roughly proportional to the polymerization degree (see Equation (15) and the

text below it). The parameter u^* always scales with the attraction range Δ according to Equation (5). It shows that u^* decreases both with Δ and with the chain stiffness defined by the Kuhn segment l . Equation (5) agrees with numerous theoretical and simulation results for polymer adsorption to an impenetrable surface [18,21,27,46,47]. Thus, although u^* must be lower for a penetrable film, the scaling relation, Equation (5), seems to be universal.

For both models, the adsorbed layer is symmetric: it is formed on both sides of the film. Generally, an adsorbed layer involves trains, loops and tails (Figure 1b). Trains are chain fragments (of length $s_{train} \gtrsim \lambda$) located mostly within the attraction layer (of thickness $\sim \Delta$). Loops are fragments between two trains located mostly outside the Δ -layer. Since the loop ends are connected to trains, they must be oriented almost tangentially to the attracting surface (with a small tilt angle θ , $\theta \lesssim \theta_\Delta \sim (\Delta/l)^{1/3}$, cf. Equation (37)). A tail is a terminal chain part with a free end (which is typically located outside the Δ -layer) whose starting point is adjacent to a train. Tails are not important for long chains above the critical point ($u > u^*$), where the adsorbed layer consists mostly of trains and loops. There are two types of loops: large semiflexible isotropic loops (of length $s \gg l$) and shorter aligned loops ($s \lesssim l$) forming two sublayers, distal ($|x| \gg l$) and proximal ($\Delta \lesssim |x| \lesssim l$), respectively. At $u \approx u^*$, aligned loops in the proximal layer show a fractal size distribution leading to an algebraic decay of polymer concentration $c(x) \propto |x|^{-\beta}$. For model ‘i’, the number density of aligned loops of length s is $\rho(s) \propto Z_l(s) \propto s^{-2}$ (Equation (11)) and $\beta = 1$ (Equation (12)). For model ‘ii’, the critical exponents depend on the area fraction w of the holes. We found that in the proximal layer, $\rho(s) \propto Z_l(s, w) \propto s^{3\alpha_1}$ (Equation (76)), where $\alpha_1 = -\frac{5}{6} + \frac{1}{\pi} \arcsin \frac{w}{2}$ (Equation (73)), and that

$$\beta = -\frac{1}{3} - 2\alpha_1 \tag{81}$$

(Equation (75)). Thus, for model ‘ii’ with $0 \leq w < 1$ we get $4/3 > \beta > 1$. For $w = 0$, the critical exponents coincide with the results for impenetrable surface [21]: $\beta = 4/3$, $3\alpha_1 = -5/2$. The opposite limit, $w \rightarrow 1$, corresponds to a perfectly permeable film. It is, therefore, not surprising that model ‘ii’ reproduces the exponents of model ‘i’ in the $w \rightarrow 1$ regime.

There is, however, a qualitative difference between the two models: Model ‘i’ is characterized by two adsorption transitions: at $u = 0$ (weak isotropic adsorption) and at $u = u^*$ (strong anisotropic adsorption). The first transition results in formation of a thick layer of long semiflexible isotropic loops. Its thickness at $0 < u \ll u^*$ is (cf. Section 4)

$$h \sim l(l/\Delta)^{1/3}u^*/u \gg l$$

However, this layer rapidly thins as u increases tending to u^* (see the first two regimes in Equation (61)). At the same time, the self-similar proximal layer of aligned loops rapidly grows so that near u^* the proximal layer (with concentration profile $c(x) \propto 1/|x|$ for $|x| \lesssim l$) becomes well-developed and dominant, marking the second transition occurring in a narrow region $|\tau| = |u/u^* - 1| \lesssim (\Delta/l)^{2/3}$. Adsorption at a symmetric interface (for a model analogous to our model ‘i’) was considered theoretically in ref. [48]. In the weak adsorption regime (apparently corresponding to u well below u^*), two length-scales characterizing the concentration profile (one $\sim l$ and another much longer) were identified [48], in qualitative agreement with our results.

By contrast, model ‘ii’ shows only one adsorption transition at $u = u^*$, leading to the formation of a self-similar proximal layer of aligned loops at $0 < \tau \lesssim (\Delta/l)^{2/3} \ll 1$. As τ is further increased, the proximal layer thins in a similar way for both models (as was established following the approach of Section 4); the thinning law for model ‘ii’ reads

$$h \sim \Delta/\tau^{3/2}, \quad 1 \gtrsim \tau \gtrsim (\Delta/l)^{2/3} \tag{82}$$

(cf. Equation (63)). The adsorbed layer thickness becomes comparable to the membrane attraction range, $h \sim \Delta$, at $\tau \sim 1$. Note that Equation (82) just slightly differs from the prediction, Equation (63), for model ‘i’: an additional log-factor, $[\ln(1/\tau)]^{3/2}$, is present in the latter case.

7.2. Notes Related to the Model of Solid Film with Holes

In Section 6, we neglected both the chain thickness d and the thickness d_m of solid parts of the membrane (shown in black in Figure 5). With finite d and d_m the chain penetration through a hole becomes slightly restricted: For geometric reasons, a penetration is possible if the tilt angle $|\theta|$ of the relevant chain segment exceeds $\theta_{min} = (d + d_m)/D$. Obviously, this condition is virtually always satisfied if the typical tilt angle $|\theta| \sim (s/l)^{1/2}$ (for a loop of length s) is much larger than θ_{min} , that is, if

$$s/l \gg (d + d_m)^2/D^2 \quad (83)$$

The latter condition defines the lower bound for the range of loop sizes where the theory of Section 6 (including the scaling relations) is applicable. Recalling that $s \ll l$, the condition (83) demands that $D \gg d + d_m$, which is always satisfied if $d + d_m \lesssim \Delta$ and $D \gg \Delta$ as assumed at the beginning of Section 6. Note also that for $D \gtrsim \lambda$ (which is equivalent to the condition $D/\sqrt{w} \gtrsim \lambda$ assumed in Section 6, provided that w is not small) and $d + d_m \lesssim \Delta$ the basic condition (83) simply follows from the condition $s \gg \lambda$, which is always required for the loops to follow a self-similar distribution in the proximal layer.

Let us turn to the size (length s) distribution of trains. For an impermeable membrane ($w \rightarrow 0$), the probability density of the train length s is nearly exponential for $s \gtrsim \lambda$. It follows from the fact that train sections of size $\Delta s \sim \lambda$ are essentially decorrelated, and hence the probability p_l that the next segment Δs escapes the attraction zone (the Δ -layer), and thus creating a (short) loop is independent of the train length. Note that by the definition of the length-scale λ , the probability $p_l \sim 1/2$, and hence the mean train length is $s_{train} \sim 2\lambda$.

For $w > 0$, the holes do not perturb the train distribution provided that the typical size of solid parts of the membrane $D_s = D/\sqrt{w} - D$ is much larger than s_{train} , $D_s \gg s_{train}$, which is equivalent to

$$D(1 - w) \gg \lambda \quad (84)$$

Thus, the train length distribution remains exponential also for a porous membrane with sufficiently large holes (obviously, this condition becomes stronger as w increases, $w \rightarrow 1$). Note, however, that the condition (84) is irrelevant to the self-similar distribution of loops considered in Section 6, which remains intact as long as $D(1 - w) \gtrsim \lambda$. It is the critical adsorption strength u^* that becomes affected by D and w in the regime $D(1 - w) \lesssim \lambda$: u^* increases as D is decreased or w is increased because the train size must be reduced here for geometric reasons.

7.3. Loop and Tail Distributions

Let us turn to the effect of the chain contour length L . Incidentally, we assumed that $L \lesssim l$ in Sections 2.2 and 2.3 where the monomer distribution in the adsorbed layers is considered using scaling arguments, while long chains, $L \gg l$, are assumed in Sections 3, 4 and 6, presenting the quantitative theory. It is noteworthy that short chains ($L \lesssim l$) cannot be trapped by a membrane at $u < u^*$: they would escape into the solution bulk. That is why we had to assume (in Sections 2.2 and 2.3) that the chain ends are forced to be located in the film. The only significant implication of this condition is that the terminal layer thickness for a moderate u is defined by the chain length, $x_{max} \sim L^{3/2}/l^{1/2}$ (cf. Equation (13)), rather than by the attraction strength u , as it happens in the case of very long chains, $L \rightarrow \infty$ (cf. Equations (61) and (63)). As a result, the distal layer is totally absent for short chains, $L \lesssim l$. However, the self-similar structure of loops in the proximal layer is virtually independent of L above u^* : it is nearly the same for $L \gg l$ and

$L \sim l$. In the general case, a finite chain length L means a finite contribution of tails to the polymer concentration profile $c(x)$. Noteworthily, the tail effect was avoided so far by either ‘pinning’ both chain ends or considering long chains, $L \rightarrow \infty$. Below, we analyze the tail effect for short chain $L \lesssim l$ pinned at only one end, thus allowing for one tail. (Instead of pinning, one can also demand a sufficiently high adsorption strength to trap the chain near the membrane; both methods give similar results).

Let $Z_1(L)$ be the total partition function of a chain (of length $\lambda \ll L \lesssim l$) with one end free and another end pinned to the membrane (with tangential orientation of the end segment), and $Z_2(L)$ be a similar partition function with the condition that both ends are located in the membrane attraction layer (allowing one end to freely glide along the surface to anneal the end-to-end distance fluctuations). Let us focus on the model ‘ii’ (solid film with holes) at the critical point $u = u^*$. The concentration due to loops at this point follows the power law, $c(x) \propto x^{-\beta}$ with $\beta > 1$. Therefore $\int c(x)dx$ is dominated by short $x \sim \Delta$, so that a finite fraction of polymer segments is inside the Δ -layers near the membrane. In this case, $Z_2(2s) \simeq \text{const } Z_2(s)^2$ since the probability to find a train (a segment of length $\gtrsim \lambda$ in contact with the membrane) near the middle of the $2s$ -chain is close to 100%. The above relation leads to $Z_2(s) \simeq \text{const } e^{\epsilon s}$, where ϵ is the adsorption energy per unit length, which must be equal to 0 by definition of the adsorption threshold u^* . Therefore, $Z_2(s) \simeq \text{const}$. Turning to $Z_1(L)$ we note that any configuration of wormlike chain (with one end pinned and another free end) can be uniquely divided in two fragments: the first one, of length $L - s$ with ends in tangential contact with the membrane, and the second, a tail of length s (with no trains in it). This decomposition leads to the following equation

$$Z_1(L) \simeq \text{const} \int_0^L Z_2(L - s)Z_t(s)ds \tag{85}$$

where $Z_t(s)$ is the tail partition function. Since a loop of length $2s$ can be considered as a combination of two tails, there is a general relation between $Z_t(s)$ and $Z_l(2s)$ (cf. ref. [21]):

$$Z_l(2s) \sim Z_t(s)^2 / (x(s)\theta(s)) \tag{86}$$

where $x(s) \propto s^{3/2}$ (cf. Equation (6)) and $\theta(s) \propto s^{1/2}$ for $s \ll l$. Recalling that $Z_l(s) \propto s^{3\alpha_1}$ (cf. Equation (76) and note that $Z_l(s) = Z_l(s, w)$ in this section, i.e., the parameter w is omitted for brevity) we obtain

$$Z_t(s) \propto s^{1+3\alpha_1/2}, s \lesssim l \tag{87}$$

where (cf. Equation (81))

$$\gamma = 1 + 3\alpha_1/2 = (3/4)(1 - \beta) \tag{88}$$

Equation (85) implies that at $u = u^*$ the statistical weight of all conformations with tail of length s is proportional to $Z_2(L - s)Z_t(s)$, and hence the tail length distribution density is

$$\rho_t(s) \simeq Z_2(L - s)Z_t(s) / \int_0^L Z_2(L - s)Z_t(s)ds \tag{89}$$

Finally, using Equation (87), we obtain (for $L \ll l$)

$$\rho_t(s) \simeq s^\gamma(\gamma + 1)/L^{\gamma+1}$$

The mean tails length $L_t = \langle s \rangle$ is then given by

$$L_t/L \simeq \frac{\gamma + 1}{\gamma + 2} = \frac{4 + 3\alpha_1}{6 + 3\alpha_1}, L \ll l$$

Recalling that $-2/3 > \alpha_1 \geq -5/6$ (cf. Equation (73)), we conclude that in critical conditions ($u = u^*$) the mass fraction of tails (L_t/L) is around 50%, and therefore it is always comparable to the mass fraction ($= (L - L_t)/L$) of loops and trains (in addition, contributions of loops and trains are obviously comparable as well). A similar argument

also shows that mass fractions of trains in the case of one pinned end (w_{train1}) and for two ends trapped near the membrane (w_{train2}) are related

$$w_{train1} \simeq \frac{1}{\gamma + 2} w_{train2} \tag{90}$$

Thus, in effect, the above results based on Equation (85) show that the tail length is typically $\sim L/2$ at $u = u^*$. The monomer distribution due to such a tail is therefore comparable with that for a single tail of length L . The latter distribution follows from Equation (6) (for $x > 0$):

$$c_t(x) \sim (l/x)^{1/3}, \quad x \lesssim x_{max}, \quad x_{max} \sim L^{3/2}/l^{1/2}, \quad L \lesssim l \tag{91}$$

(Note that here and below we define $c_t(x)$ in such a way that $c_t(x)dx$ is the mean length of tail segments in the layer $(x, x + dx)$; a similar definition applies to $c_l(x)$ for loops and trains). At $u = u^*$, the concentration contribution of loops/trains is

$$c_l(x) \sim \frac{L}{\Delta} \left(\frac{\Delta}{x}\right)^\beta, \quad \Delta \lesssim x \lesssim x_{max} \tag{92}$$

where β is defined in Equation (81) (cf. also Equation (75)). The prefactor in Equation (92) can be obtained from the condition of nearly equal masses of loops/trains and tails, $\int c_l(x)dx \sim \int c_t(x)dx \sim L/2$, as discussed above. Note also that both c_t and c_l vanish exponentially at $x > x_{max}$.

Obviously, loops dominate at short distances, while tails are more important at the periphery:

$$c(x) \sim \begin{cases} c_l(x), & \Delta < x < x^* \\ c_t(x), & x_{max} \gtrsim x > x^* \end{cases} \tag{93}$$

where $c(x) = c_l(x) + c_t(x)$ is the total concentration, and

$$x^* \sim \Delta(L/\lambda)^{1/(\beta-1/3)} \sim \Delta(x_{max}/\Delta)^{2/(3\beta-1)} \tag{94}$$

is the crossover distance; $\Delta \ll x^* < x_{max}$ since $3\beta - 1 > 2$ and $L \gg \lambda$. (Note that we do not consider trains any more focusing on the regime $x > \Delta$; it must be always kept in mind that an equivalent adsorbed layer at $x < -\Delta$ is also present). Equation (94) is applicable for short chains, $L \lesssim l$. For $L \sim l$, it gives

$$x^* \sim l(\Delta/l)^{\frac{\beta-1}{\beta-1/3}} \gtrsim l^{2/3}\Delta^{1/3} \tag{95}$$

Qualitatively the same picture stays valid also for longer chains, $L \gg l$. In this case, the chain behaves flexibly at length scales $x \gg l$, so $x_{max} \sim (Ll)^{1/2}$ (i.e., x_{max} is defined by the coil size R , Equation (3)). At the critical adsorption point ($u = u^*$), the concentration contribution of semiflexible isotropic loops is nearly constant in the regime $x \gg l$ (following the classical results on the ideal flexible chain adsorption [4]):

$$c_l(x) \sim \begin{cases} c_0, & x_{max} \sim (Ll)^{1/2} > x > l \\ c_0(l/x)^\beta, & \Delta < x < l \end{cases} \tag{96}$$

where $c_0 \sim L/(\sqrt{Ll} + l^\beta \Delta^{1-\beta})$ is found from the basic principle that total masses of loops and tails are always comparable at $u = u^*$.

As for the tails, their monomer concentration profile is defined in Equation (91) for $x \lesssim l$, while $c_t(x) \propto x$ for $x \gtrsim l$ (note that the membrane acts as a repulsive surface

for long semiflexible tails since by definition the tail monomers never enter the surface attraction zone):

$$c_t(x) \sim \begin{cases} x/l, & x_{max} > x > l \\ (l/x)^{1/3}, & \Delta < x < l \end{cases} \tag{97}$$

Note that the scaling law, $c_t(x) \propto x$ at $x \gg l$ (valid for a tail emanating from a repulsive surface) comes from a simple argument already used to derive Equation (91): $c_t(x) \sim \frac{s/2}{x/2}$, where $s/2$ is the length of tail fragment between points $s/2$ and s along its contour, and $x/2$ is the thickness of the layer where this fragment is typically located spanning distances between $x/2$ and x , with $x \sim \sqrt{s l}$ being its typical size, cf. Equation (3).

Using Equations (96) and (97), we find that monomers in the loops dominate at $x < x^*$, and tail monomers - at $x > x^*$ (cf. Equation (93)), where

$$x^* \sim \begin{cases} l[L/(l^\beta \Delta^{1-\beta})]^{1/(\beta-1/3)}, & L < l^\beta \Delta^{1-\beta} \\ lL/(\sqrt{lL} + l^\beta \Delta^{1-\beta}), & L > l^\beta \Delta^{1-\beta} \end{cases} \tag{98}$$

Thus, the tail contribution in the proximal layer can be totally neglected if $L \gg L^* \sim l^\beta \Delta^{1-\beta}$. Note that $L^* \gg l$ since $\beta > 1$. The obtained results can be applied to the case of an impenetrable surface as well by setting $\beta = 4/3$ ($\alpha_1 = -5/6$). The crossover distance x^* always increases with L (cf. Equations (94) and (98)).

The energy E of the polymer/membrane complex is proportional to the number of polymer/surface contacts (n_c) or, in other words, to the total polymer length L_c in the attractive layers of thickness Δ ,

$$L_c = 2 \int_0^\Delta c(x) dx \sim c(\Delta) \Delta$$

Taking into account that $c(\Delta) \sim c_l(\Delta)$ and using Equations (92) and (96), we obtain L_c at the critical point $u = u^*$:

$$L_c \sim \begin{cases} L/2, & L < \tilde{L} \\ \sqrt{L\tilde{L}}, & L > \tilde{L} \end{cases} \tag{99}$$

where the crossover length \tilde{L} is

$$\tilde{L} \sim l(l/\Delta)^{2(\beta-1)} \gg L^* \gg l \tag{100}$$

The fraction $p = L_c/L$ of trapped monomers, therefore, is (cf. Equation (59)):

$$p \sim \begin{cases} 0.5, & L < \tilde{L} \\ \sqrt{\tilde{L}/L}, & L > \tilde{L} \end{cases} \tag{101}$$

Equation (99) shows that the contact exponent ϕ (cf. Equation (1)) changes from $\phi = 1$ for relatively short chains ($L \ll \tilde{L}$) to $\phi = 1/2$ for longer chains ($L \gg \tilde{L}$). It is remarkable that $\phi = 1$ is thus predicted also for semiflexible chains ($\tilde{L} \gg L \gg l$) forming a complicated structure of competing long loops, aligned loops and tails. The result, $\phi = 1/2$, for very long chains ($L \rightarrow \infty$) trivially corresponds to the well-known critical behavior of ideal flexible polymers [4]. However, even in this long-chain limit, the amount of contacts rapidly increases from $L_c \propto L^{1/2}$ to the maximum $L_c \sim L$ as the membrane attraction strength increases above u^* . Indeed, at $u > u^*$, the adsorption free energy ϵ is positive (cf. Equation (34)), so the loops and tails of length $s \gg 1/\epsilon$ are exponentially suppressed (cf. Equation (26)). Therefore, the concentration profile for $L \rightarrow \infty$ at a given $\tau = u/u^* - 1 > 0$

becomes roughly equivalent to the profile of loops at the critical point for $L \sim 1/\epsilon$, where $\epsilon = \epsilon(\tau)$. Using Equation (101) we thus obtain:

$$p \sim \begin{cases} 0.5 & , \epsilon \tilde{L} > 1 \\ \sqrt{\epsilon \tilde{L}} & , \epsilon \tilde{L} < 1 \end{cases} \tag{102}$$

It remains to find out how ϵ depends on the deviation $\tau = u/u^* - 1 > 0$ from the critical point. Using Equations (25) and (102) we obtain the following as a result:

$$\epsilon \sim \begin{cases} \tau^2 \tilde{L} (u^*)^2 & , \tau \lesssim \tau^* \\ \tau u^* & , \tau \gtrsim \tau^* \end{cases} \tag{103}$$

$$p \sim \begin{cases} \tau/\tau^* & , \tau \lesssim \tau^* \\ 0.5 & , \tau \gtrsim \tau^* \end{cases} \tag{104}$$

where $\tau^* \sim 1/(u^* \tilde{L}) \sim \lambda/\tilde{L} \sim (\Delta/l)^{2\beta-4/3}$. Note that $\tau^* \ll 1$ since $2/3 < 2\beta - 4/3 \leq 4/3$. Equation (104) therefore shows that a small increase of u from u^* to $u^*(1 + \tau^*)$ leads to a strong increase of the contact fraction p from 0 to $p \sim 1$ implying that $L_c \sim L$ as stated above. The terminal thickness h of the adsorbed layer is nearly equal to the extension (in the direction perpendicular to the membrane) of the terminal loops of contour length $s \sim 1/\epsilon$. Thus, using Equation (103) we obtain

$$h \sim \begin{cases} l(\Delta/l)^{\beta-1/3} \tau^{-1} & , 0 < \tau < \tau^* \\ l(\Delta/l)^{1/3} \tau^{-1/2} & , \tau^* < \tau < \tau^{**} \\ \Delta/\tau^{3/2} & , \tau^{**} < \tau < 1 \end{cases} \tag{105}$$

where $\tau^{**} \sim \delta^2 = (\Delta/l)^{2/3}$. In particular, we get $h \sim l$ for $\tau \sim \tau^{**}$. Therefore, the distal layer is suppressed at $\tau > \tau^{**}$.

7.4. Non-Ideality Effects

In this study, we assumed no interactions between polymer segments. This assumption is justified for a sufficiently small ratio of polymer chain thickness d to its Kuhn segment l , $d/l \ll 1$, which ensures that the volume fraction occupied by a single chain is low. The bottleneck for this assumption occurs in the contact Δ -layer near the membrane, where the polymer concentration (volume fraction c_ϕ) increases in the adsorbed state ($u \geq u^*$). The maximum polymer volume fraction c_ϕ there can be estimated as $c_\phi \sim Ld^2/(\Delta R^2) \sim d^2/(l\Delta)$, where R is the coil size defined in Equation (3). The excluded-volume interaction free energy per Kuhn segment is $U_l \sim Tc_\phi l/d \sim Td/\Delta$ [49]. Therefore, for $\Delta \gg d$, the interactions are rather weak, $U_l \ll T$, and can be neglected for the adsorption profile $c(x)$ and the contact fraction p (at least, in the most interesting regime $\tau \gg \delta^2 d/\Delta$). By contrast, interactions of segments are important if the membrane potential is very short-range, $\Delta \lesssim d$. In this case, the adsorbed chain size in the yz -plane must be significantly swollen compared to the ideal size, Equation (3). This effect was observed in simulation studies [27,50,51] and experimentally for DNA molecules electrostatically bound to cationic lipid bilayers [10]. (Note that the two-dimensional swelling effect leads to a decrease in c_ϕ and, therefore, to a lower free energy contribution due to interactions). In both cases, however, the interactions between monomers either in the Δ -layer or outside it are just marginally important for the statistics of long loops (provided that the Fixman parameter $z_F \sim (d/l)(L/l)^{1/2}$ [52] is sufficiently low, that is $L \ll l^3/d^2$). The main effect of the interactions for the adsorption transition then reduces to some renormalization (an increase) of the critical adsorption strength u^* .

7.5. Estimates of the Layer Thickness

Here, we provide some estimates on the distance range corresponding to the self-similar structure of aligned loops (which is the most interesting part of the adsorbed layer

at the critical point) for some hypothetical polymer/membrane systems. As examples, let us consider two types of membranes: a typical phospholipid membrane of effective thickness $2\Delta \sim 8$ nm in water and a porous carbon nano-membrane of thickness $d_m \sim 1$ nm with holes of diameter $D \sim 10$ nm [45]. As polymers, we can consider a double-strand DNA (with thickness $d \sim 2$ nm and Kuhn segment $l = 2l_p \sim 100$ nm) and chitosan with $d \sim 1$ nm and $l = 2l_p \sim 90$ nm (at a low salt concentration $c_s = 1.25$ mM [53]; l_p for chitosan decreases at higher c_s) in aqueous solutions. The case of lipid membrane roughly corresponds to the model of Sections 2.2 and 3 (here, we set aside issues related to whether polymer penetration through the membrane is kinetically allowed or not), so the self-similar sublayer is expected in the distance range $\Delta < |x| < l$ which corresponds to $4 \text{ nm} < |x| < 100 \text{ nm}$ for both polymers. For the porous carbon nano-membrane in water, the attraction range is defined mostly by the Debye length r_D , $\Delta \sim r_D$. This Δ should be compared with $x_{min} \sim D^{3/2}/l^{1/2}$ for a moderate porosity $w \sim 0.5$ (cf. Section 6). For both polymers (DNA and chitosan), we thus arrive at $x_{min} \sim 3$ nm. In the case of DNA adsorption, we assume physiological ionic strength, $c_s \approx 0.15$ M, so $\Delta \sim r_D \sim 1$ nm. Therefore, for the DNA adsorption onto the carbon membrane $x_{min} > r_D$, and hence a self-similar structure of loops is predicted for $x_{min} < |x| < l$, i.e., for $3 \text{ nm} < |x| < 100 \text{ nm}$. By contrast, for chitosan adsorption (at $c_s = 1.25$ mM) the screening length is much longer, $r_D \sim 9$ nm, hence $r_D > x_{min}$ and the sublayer of aligned loops corresponds to $r_D < |x| < l$, i.e., to $|x|$ between 10 and 100 nm.

8. Summary

We theoretically analyzed adsorption of a stiff wormlike polymer chain (with large persistence length) on permeable and semi-permeable free-standing flat nano-membranes. The membrane attraction length-range Δ is assumed to be much shorter than the polymer Kuhn segment l . Two membrane models are considered: In the first case, adsorption is driven by monomer attraction to a uniform membrane (modeled as a short-range potential field). A nanoporous solid film whose surface attracts polymer segments is studied as the second model (its relevant example is described in ref. [45]). In both cases, we predict the formation of a fractal proximal layer of aligned polymer loops at the critical strength u^* of monomer/film attraction (u^* is approximately given by Equation (5) for both models). The monomer concentration c strongly increases near the membrane according to a power law $c(x) \propto x^{-\beta}$ in the proximal layer. It is shown that the critical exponent β for the first model ($\beta = 1$) is different from the value obtained for adsorption to an impenetrable surface ($\beta = 4/3$). For the second model, we demonstrate that β depends on the area fraction of holes, w ; the universal asymptotically exact dependence $\beta = \beta(w)$ is obtained analytically (cf. Equation (81)). Moreover, we characterize both spatial and orientational distributions of polymer segments in the proximal layer in an asymptotically exact way.

We established that generally, the adsorbed layer is characterized by a complex structure involving (on each side of the membrane) the thin contact Δ -layer of trapped segments, the fractal proximal layer of thickness comparable with l (or smaller at $u > u^*$), and the distal layer of long semiflexible loops. Moreover, polymer loops and tails can compete in both proximal and distal layers. We found that for the first model, the distal layer is suppressed already at $u = u^*$, while for the second model, this happens slightly above the threshold u^* , at $u/u^* - 1 \sim (\Delta/l)^{2/3}$ (cf. Equation (105)). At a higher attraction strength u for both models, the adsorbed layers can be viewed as a fractal distribution of loops. It is also shown that the fraction p of trapped chain segments in contact with the membrane becomes significant, $p \sim 0.5$, for $u/u^* - 1 \gtrsim (\Delta/l)^{2\beta-4/3}$, again for both models.

Turning to the contribution of polymer tails, we established that it is not important for very long chains. However, in the general case of finite chain length L , the tails can dominate the adsorbed polymer concentration profile at large distances, $x > x^*$, while loops dominate closer to the membrane. Near the adsorption threshold, $u \approx u^*$, the crossover distance x^* increases with L as $x^* \propto L^{1/(\beta-1/3)}$ for $L < L^*$, $x^* \propto L$ for $L^* < L < (L^*)^2/l$, and $x^* \propto \sqrt{L}$ for $L > (L^*)^2/l$, where $L^* \sim l(l/\Delta)^{\beta-1}$ (cf. Equation (98)). As a side product,

we obtained the generating function of the probability distribution of the number of intersections between a geometric plane and a wormlike chain, whose ends are tangentially attached to the plane (cf. Equation (78)).

We thus provide a powerful theoretical method (including both the quantitative transfer-matrix approach and scaling concepts) to study the microstructure of adsorbed wormlike polymer layers. The current work is therefore likely to open new perspectives in predicting the physical properties of various polymer/membrane complexes. The significance of the obtained results is underlined by the facts that semiflexible polymers are often used in applications to modify the properties of membranes and films and to tune the interfacial properties of functional layers [1–7,33,34], that the adsorption of semiflexible macromolecules on substrates is involved in many biological processes [8,9], that important biopolymers, such as double-strand DNA, polypeptides and protein biofilaments, can be roughly described by the wormlike chain model [10,25,26,54,55], and that their interactions with cell membranes are of key interest in understanding various biological functions of living systems [8–11,34–38].

Author Contributions: Conceptualization, A.S.; investigation, All authors; writing—original draft preparation, All authors. All authors have read and agreed to the published version of the manuscript.

Funding: This research was partially funded by ANR grant ‘MONA_LISA’.

Institutional Review Board Statement: Not applicable.

Informed Consent Statement: Not applicable.

Data Availability Statement: Not applicable.

Conflicts of Interest: The authors declare no conflict of interest.

Nomenclature

c	Polymer concentration
$c(x)$	Monomer concentration profile
$c_l(x)$	Concentration profile of monomers belonging to loops
$c_t(x)$	Concentration profile of monomers belonging to tails
D	Mean hole diameter
E	Chain potential energy
F_{conf}	Chain confinement free energy
$f(\eta)$	Angle-dependent factor of the partition function, Equation (39)
h	The terminal thickness of adsorbed layer
L	Chain contour length
L_c	The total polymer length in the attractive layer
L_t	The mean tail length
l_p	Persistence length
l	Kuhn segment
N	Number of monomer units (or λ -segments) per chain
n_c	Number of polymer/membrane contacts
p	Fraction of polymer segments in the attraction layer, Equation (59)
R	Coil size
T	Temperature in energy units
U	Attraction potential (per unit length), Equation (4)
u	Membrane attraction strength
u^*	Critical adsorption threshold
w	Porosity of nano-membrane
$ x $	Distance to the membrane
$\tilde{x}, x^*, \tilde{L}$	Crossover length-scales
$Z_l(s)$	Partition function of a loop of length s
$Z_t(s)$	Partition function of a tail of length s
$Z_l(s, w)$	Partition function of a loop s for porosity w , Equation (70)

α	Critical exponent, Equation (39)
α_0	The value of α corresponding to a repulsive membrane
α_1	The exponent corresponding to critically adsorbing membrane
β	Critical exponent for proximal concentration profile, Equation (81)
Δ	Membrane attraction range
ϵ	Reduced adsorption energy per unit length, Equation (34)
η	Reduced tilt angle, $\eta = \theta/\theta_x$
θ_x	Typical bending angle of a loop at distance x from the film
Λ	Crossover length-scale
λ	Characteristic segment length in the contact layer, Equation (7)
$\rho(\eta)$	Distribution of the reduced tilt angle, Equation (48)
τ	Relative deviation from the critical point, $\tau = u/u^* - 1$
ϕ	The crossover critical exponent, Equation (1)
ψ	The chain partition function
Ψ	The Tricomi function, Equation (43)

References

- Napper, D.H. *Polymer Stabilization of Colloidal Dispersions*; Academic Press: London, UK, 1983.
- Lekkerkerker, H.; Tuinier, R. *Colloids and Depletion Interaction*; Springer: Berlin/Heidelberg, Germany, 2011.
- De Gennes, P.G. Polymers at an Interface; a Simplified View. *Adv. Colloid Interface Sci.* **1987**, *27*, 189–209. [[CrossRef](#)]
- Eisenriegler, E. *Polymers Near Surfaces*; World Scientific: Singapore, 1993.
- Cohen-Stuart, M.; Cosgrove, T.; Vincent, B. Experimental aspects of polymer adsorption at solid/solution interface. *Adv. Colloid Interface Sci.* **1985**, *24*, 143–239. [[CrossRef](#)]
- Barnett, K.; Cosgrove, T.; Crowley, T.; Tadros, J.; Vincent, B. *The Effects of Polymers on Dispersion Stability*; Tadros, J., Ed.; Academic Press: London, UK, 1982; p. 183.
- Semenov, A.N.; Shvets, A.A. Theory of colloid depletion stabilization by unattached and adsorbed polymers. *Soft Matter* **2015**, *11*, 8863–8878. [[CrossRef](#)] [[PubMed](#)]
- Li, B.; Abel, S.M. Shaping membrane vesicles by adsorption of a semiflexible polymer. *Soft Matter* **2018**, *14*, 185–193. [[CrossRef](#)] [[PubMed](#)]
- Goda, T.; Goto, Y.; Ishihara, K. Cell-penetrating macromolecules: Direct penetration of amphipathic phospholipid polymers across plasma membrane of living cells. *Biomaterials* **2010**, *31*, 2380–2387. [[CrossRef](#)]
- Maier, B.; Radler, J.O. Conformation and Self-Diffusion of Single DNA Molecules Confined to Two Dimensions. *Phys. Rev. Lett.* **1999**, *82*, 1911–1914. [[CrossRef](#)]
- Herold, C.; Schwille, P.; Petrov, E.P. DNA Condensation at Freestanding Cationic Lipid Bilayers. *Phys. Rev. Lett.* **2010**, *104*, 148102. [[CrossRef](#)]
- Binder, K. Critical Behaviour at Surfaces. In *Phase Transitions and Critical Phenomena*; Domb, C., Lebowitz, J.L., Eds.; Academic Press: London, UK, 1983; Volume 8, p. 1.
- Fisher, M.E. Walks, walls, wetting, and melting. *J. Stat. Phys.* **1984**, *34*, 667–729. [[CrossRef](#)]
- Martins, P.H.L.; Plascak, J.A.; Bachmann, M. Adsorption of flexible polymer chains on a surface: Effects of different solvent conditions. *J. Chem. Phys.* **2018**, *148*, 204901. [[CrossRef](#)]
- Taylor, M.P.; Basnet, S.; Luettmer-Strathmann, J. Partition-function-zero analysis of polymer adsorption for a continuum chain model. *Phys. Rev. E* **2021**, *104*, 034502. [[CrossRef](#)]
- Grassberger, P. Simulations of grafted polymers in a good solvent. *J. Phys. A Math. Gen.* **2005**, *38*, 323–331. [[CrossRef](#)]
- Zinn-Justin, J. *Quantum Field Theory and Critical Phenomena*; Clarendon Press: Oxford, UK, 1989.
- Maggs, A.C.; Huse, D.A.; Leibler, S. Unbinding Transitions of Semi-flexible Polymers. *Europhys. Lett.* **1989**, *8*, 615–620. [[CrossRef](#)]
- Khokhlov, A.R.; Ternovsky, F.F.; Zheligovskaya, E.A. Statistics of stiff polymer chains near an adsorbing surface. *Makromol. Chem. Theory Simul.* **1993**, *2*, 151. [[CrossRef](#)]
- Kuznetsov, D.V.; Sung, W. Semiflexible Polymers near Attracting Surfaces. *Macromolecules* **1998**, *31*, 2679–2682. [[CrossRef](#)]
- Semenov, A.N. Adsorption of a semiflexible wormlike chain. *Eur. Phys. J. E* **2002**, *9*, 353–363. [[CrossRef](#)]
- Odjik, T. The statistics and dynamics of confined or entangled stiff polymers. *Macromolecules* **1983**, *16*, 1340. [[CrossRef](#)]
- Baschnagel, J.; Meyer, H.; Wittmer, J.; Kulić, I.; Mohrbach, H.; Ziebert, F.; Nam, G.M.; Lee, N.K.; Johner, A. Semiflexible Chains at Surfaces: Worm-Like Chains and beyond. *Polymers* **2016**, *8*, 286. [[CrossRef](#)]
- Kratky, O.; Porod, G. Röntgenuntersuchung gelöster Fadenmoleküle. *Rec. Trav. Chim.* **1949**, *68*, 1106. [[CrossRef](#)]
- Bezanilla, M.; Drake, B.; Nudler, E.; Kashlev, M.; Hansma, P.K.; Hansma, H.G. Motion and enzymatic degradation of DNA in the atomic force microscope. *Biophys. J.* **1994**, *67*, 2454–2459. [[CrossRef](#)]
- Bustamante, C.; Rivetti, C. Visualizing Protein-Nucleic Acid Interactions on a Large Scale with the Scanning Force Microscope. *Annu. Rev. Biophys. Biomol. Struct.* **1996**, *25*, 395–429. [[CrossRef](#)]
- Milchev, A.; Binder, K. How does stiffness of polymer chains affect their adsorption transition? *J. Chem. Phys.* **2020**, *152*, 064901. [[CrossRef](#)] [[PubMed](#)]

28. Landau, L.D.; Lifshitz, E.M. *Statistical Physics*; Pergamon Press: Oxford, UK, 1998.
29. Grosberg, A.Y. On Some Possible Conformational States of Homogeneous Elastic Polymer Chain. *Biofizika* **1979**, *24*, 30–36.
30. Edwards, S.F. The statistical mechanics of polymers with excluded volume. *Proc. Phys. Soc.* **1965**, *85*, 613. [[CrossRef](#)]
31. Grosberg, A.; Khokhlov, A. *Statistical Physics of Macromolecules*; American Institute of Physics: New York, NY, USA, 1994.
32. De Gennes, P.G. *Scaling Concepts in Polymer Physics*; Cornell Univ. Press: Ithaca, NY, USA; London, UK, 1985.
33. Antonietti, M.; Kaul, A.; Thünemann, A. Complexation of lecithin with cationic polyelectrolytes. *Langmuir* **1995**, *11*, 2633. [[CrossRef](#)]
34. McLaughlin, S.A. Electrostatic Potentials at Membrane-Solution Interfaces. *Curr. Top. Membr. Transp.* **1977**, *9*, 71–144.
35. Dubnau, D.A. DNA Uptake in Bacteria. *Annu. Rev. Microbiol.* **1999**, *53*, 217–244. [[CrossRef](#)]
36. Wolff, J.A.; Budker, V. The mechanism of naked DNA uptake and expression. *Adv. Genet.* **2005**, *54*, 3–20.
37. Howorka, S. Building membrane nanopores. *Nat. Nanotechnol.* **2017**, *12*, 619–630. [[CrossRef](#)]
38. Arkhangelsky, E.; Sefi, Y.; Hajaj, B.; Rothenberg, G.; Gitis, V. Kinetics and mechanism of plasmid DNA penetration through nanopores. *J. Membr. Sci.* **2011**, *371*, 45–51. [[CrossRef](#)]
39. Jia, P.; Zuber, K.; Guo, Q.; Gibson, B.C.; Yang, J.; Eberndorff-Heidepriem, H. Large-area Freestanding Gold Nanomembranes with Nanoholes. *Mater. Horiz.* **2019**, *6*, 1005. [[CrossRef](#)]
40. Winter, A.; Ekinici, Y.; Götzhäuser, A.; Turchanin, A. Freestanding carbon nanomembranes and graphene monolayers nanopatterned via EUV interference lithography. *2D Mater.* **2019**, *6*, 021002. [[CrossRef](#)]
41. Schuster, C.; Rodler, A.; Tscheliessnig, R.; Jungbauer, A. Freely suspended perforated polymer nanomembranes for protein separations. *Sci. Rep.* **2018**, *8*, 4410. [[CrossRef](#)]
42. Manoharan, M.P.; Lee, H.; Rajagopalan, R.; Foley, H.C.; Haque, M.A. Elastic Properties of 4–6 nm thick Glassy Carbon Thin Films. *Nanoscale Res. Lett.* **2010**, *5*, 14–19. [[CrossRef](#)]
43. Angelova, P.; Götzhäuser, A. Carbon Nanomembranes. *Phys. Sci. Rev.* **2017**, *2*, 20160105.
44. Garcia-Vidal, F.J.; Martin-Moreno, L.; Pendry, J.B. Surfaces with holes in them: new plasmonic metamaterials. *J. Opt. A Pure Appl. Opt.* **2005**, *7*, S97–S101. [[CrossRef](#)]
45. Ritter, R.; Wilhelm, R.A.; Stöger-Pollach, M.; Heller, R.; Mücklich, A.; Werner, U.; Vieker, H.; Beyer, A.; Facsko, S.; Götzhäuser, A.; Aumayr, F. Fabrication of nanopores in 1nm thick carbon nanomembranes with slow highly charged ions. *Appl. Phys. Lett.* **2013**, *102*, 063112. [[CrossRef](#)]
46. Gompper, G.; Seifert, U. Unbinding transition of flexible Gaussian polymers in two dimensions. *J. Phys. A Math. Gen.* **1990**, *23*, L1161. [[CrossRef](#)]
47. Kierfeld, J.; Lipowsky, R. Unbinding and desorption of semiflexible polymers. *Europhys. Lett.* **2003**, *62*, 285. [[CrossRef](#)]
48. Stepanow, S. Adsorption of a semiflexible polymer onto interfaces and surfaces. *J. Chem. Phys.* **2001**, *115*, 1565. [[CrossRef](#)]
49. Semenov, A.N.; Khokhlov, A.R. Statistical physics of liquid-crystalline polymers. *Sov. Phys. Uspekhi* **1988**, *31*, 988–1014. [[CrossRef](#)]
50. Milchev, A.; Binder, K. Semiflexible Polymers Interacting With Planar Surfaces: Weak versus Strong Adsorption. *Polymers* **2020**, *12*, 255. [[CrossRef](#)] [[PubMed](#)]
51. Milchev, A.; Binder, K. Linear Dimensions of Adsorbed Semiflexible Polymers: What Can Be Learned about Their Persistence Length? *Phys. Rev. Lett.* **2019**, *123*, 128003. [[CrossRef](#)] [[PubMed](#)]
52. Semenov, A.N.; Nyrkova, I.A. Statistical Description of Chain Molecules. In *Polymer Science: A Comprehensive Reference*; Matyjaszewski, K., Moeller, M., Eds.; Elsevier BV: Amsterdam, The Netherlands, 2012; Volume 1, pp. 3–29.
53. Kang, Y.; Zhao, X.; Han, X.; Ji, X.; Chen, Q.; Pasch, H.; Liu, Y. Conformation and persistence length of chitosan in aqueous solutions of different ionic strengths via asymmetric flow field-flow fractionation. *Carbohydr. Polym.* **2021**, *271*, 118402. [[CrossRef](#)] [[PubMed](#)]
54. Fletcher, D.A.; Mullins, R.D. Cell mechanics and the cytoskeleton. *Nature* **2010**, *463*, 485–492. [[CrossRef](#)] [[PubMed](#)]
55. Abels, J.A.; Moreno-Herrero, F.; van der Heijden, T.; Dekker, C.; Dekker, N.H. Single-Molecule Measurements of the Persistence Length of Double-Stranded RNA. *Biophys. J.* **2005**, *88*, 2737–2744. [[CrossRef](#)]

Disclaimer/Publisher’s Note: The statements, opinions and data contained in all publications are solely those of the individual author(s) and contributor(s) and not of MDPI and/or the editor(s). MDPI and/or the editor(s) disclaim responsibility for any injury to people or property resulting from any ideas, methods, instructions or products referred to in the content.